REVIEW ARTICLE

How Well Do We Understand and Evaluate Climate Change Feedback Processes?

Sandrine Bony,[a] Robert Colman,[b] Vladimir M. Kattsov,[c] Richard P. Allan,[d]
Christopher S. Bretherton,[e] Jean-Louis Dufresne,[a] Alex Hall,[f] Stephane Hallegatte,[g]
Marika M. Holland,[h] William Ingram,[i] David A. Randall,[j] Brian J. Soden,[k] George Tselioudis,[l]
and Mark J. Webb[m]

[a] Laboratoire de Météorologie Dynamique, IPSL, CNRS, Paris, France
[b] Bureau of Meteorology Research Centre, Melbourne, Australia
[c] Voeikov Main Geophysical Observatory, St. Petersburg, Russia
[d] Environmental Systems Science Centre, University of Reading, Reading, United Kingdom
[e] Department of Atmospheric Sciences, University of Washington, Seattle, Washington
[f] Department of Atmospheric and Oceanic Sciences, University of California, Los Angeles, Los Angeles, California
[g] Centre International de Recherche sur l'Environnement et le Développement, Nogent-sur-Marne, and Centre National de Recherches Météorologiques, Météo-France, Toulouse, France
[h] National Center for Atmospheric Research, Boulder, Colorado
[i] Atmospheric, Oceanic and Planetary Physics, Clarendon Laboratory, Oxford, and Hadley Centre for Climate Prediction and Research, Met Office, Exeter, United Kingdom
[j] Department of Atmospheric Science, Colorado State University, Fort Collins, Colorado
[k] Rosenstiel School of Marine and Atmospheric Science, University of Miami, Miami, Florida
[l] NASA GISS, and Department of Applied Physics, Columbia University, New York, New York
[m] Hadley Centre for Climate Prediction and Research, Met Office, Exeter, United Kingdom

ABSTRACT

Processes in the climate system that can either amplify or dampen the climate response to an external perturbation are referred to as climate feedbacks. Climate sensitivity estimates depend critically on radiative feedbacks associated with water vapor, lapse rate, clouds, snow, and sea ice, and global estimates of these feedbacks differ among general circulation models. By reviewing recent observational, numerical, and theoretical studies, this paper shows that there has been progress since the Third Assessment Report of the Intergovernmental Panel on Climate Change in (i) the understanding of the physical mechanisms involved in these feedbacks, (ii) the interpretation of intermodel differences in global estimates of these feedbacks, and (iii) the development of methodologies of evaluation of these feedbacks (or of some components) using observations. This suggests that continuing developments in climate feedback research will progressively help make it possible to constrain the GCMs' range of climate feedbacks and climate sensitivity through an ensemble of diagnostics based on physical understanding and observations.

1. Introduction

The global mean surface air temperature change in response to a doubling of the atmospheric CO_2 concentration, commonly referred to as the climate sensitivity, plays a central role in climate change studies. According to the Third Assessment Report (TAR) of the In-

tergovernmental Panel on Climate Change (IPCC), the equilibrium climate sensitivity[1] estimates from general circulation models (GCMs) used for climate change projections range from 2° to 5°C (Houghton et al. 2001). This range, which constitutes a major source of uncertainty for climate stabilization scenarios (Caldeira et al. 2003), and which could in fact be even larger

---

[1] "Equilibrium climate sensitivity" refers to the global mean surface air temperature change experienced by the climate system after it has attained a new equilibrium in response to a doubling of the atmospheric carbon dioxide concentration.

Corresponding author address: Sandrine Bony, LMD/IPSL, Boite 99, 4 Place Jussieu, 75252 Paris CEDEX 05, France.
E-mail: bony@lmd.jussieu.fr

(Murphy et al. 2004; Stainforth et al. 2005), principally arises from differences in the processes internal to the climate system that either amplify or dampen the climate system's response to the external forcing [(National Research Council) NRC (2003)]. These processes are referred to as climate feedbacks (see appendix A for a more formal definition of climate feedbacks).

Every climate variable that responds to a change in global mean surface temperature through physical or chemical processes and that directly or indirectly affects the earth's radiation budget has the potential to constitute a climate change feedback. In this paper, we focus on the feedbacks associated with climate variables (i) that *directly* affect the top-of-the-atmosphere (TOA) radiation budget, and (ii) that respond to surface temperature mostly through *physical* (rather than chemical or biochemical) processes. We will thus focus on the radiative feedbacks associated with the interaction of the earth's radiation budget with water vapor, clouds, temperature lapse rate, and surface albedo in snow and sea ice regions, whose role in GCM estimates of equilibrium climate sensitivity has been widely established. On the other hand, we will not consider the feedbacks associated with the response to temperature of the carbon cycle or of aerosols and trace gases, nor those associated with soil moisture changes or ocean processes, although these processes might have a substantial impact on the magnitude, the pattern, or the timing of climate warming (NRC 2003).

Water vapor constitutes a powerful greenhouse gas, and therefore an increase of water vapor with temperature will oppose the increase in radiative cooling due to increasing temperature, and so constitute a positive feedback. The earth's cryosphere reflects part of the incoming shortwave (SW) radiation to space, and therefore the melting of snow and sea ice with rising temperature constitutes another positive feedback. The temperature lapse rate in the troposphere (i.e., the rate of decrease of atmospheric temperature with height) affects the atmospheric emission of longwave (LW) radiation to space, and thus the earth's greenhouse effect (the stronger the decrease of temperature with height, the larger the greenhouse effect). Therefore, an atmospheric warming that is larger (smaller) in the upper troposphere than at low levels produces a negative (positive) radiative feedback compared to a uniform temperature change. Clouds strongly modulate the earth's radiation budget, and a change in their radiative effect in response to a global temperature change may produce a substantial feedback on the earth's temperature. But the sign and the magnitude of the global mean
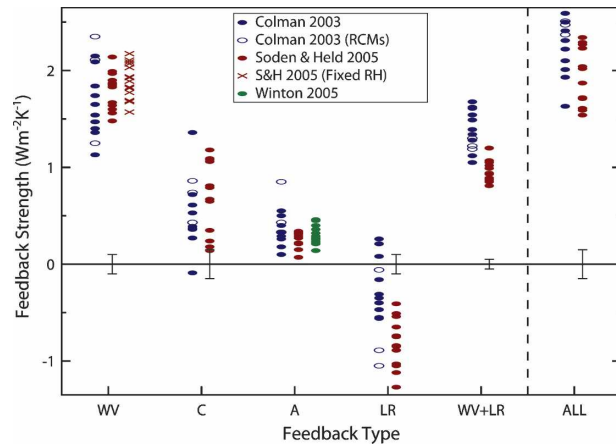

FIG. 1. Comparison of GCM climate feedback parameters (in W m^{-1} K^{-1}) for water vapor (WV), cloud (C), surface albedo (A), lapse rate (LR), and the combined water vapor + lapse rate (WV + LR). ALL represents the sum of all feedbacks. Results are taken from Colman (2003; in blue), Soden and Held (2006, in red), and Winton (2006, in green). Closed and open symbols from Colman (2003) represent calculations determined using the PRP and the RCM approaches, respectively. Crosses represent the water vapor feedback computed for each model from Soden and Held (2006) assuming no change in relative humidity. Vertical bars depict the estimated uncertainty in the calculation of the feedbacks from Soden and Held (2006).

cloud feedback depends on so many factors that it remains very uncertain.

Several approaches have been proposed to diagnose global radiative feedbacks in GCMs (appendix B), each of these having its own strengths and weaknesses (Soden et al. 2004; Stephens 2005). Since the TAR, some of them have been applied to a wide range of GCMs, which makes it possible to compare the feedbacks produced by the different models and then to better interpret the spread of GCMs' estimates of climate sensitivity.

Figure 1 compares the quantitative estimates of global climate feedbacks (decomposed into water vapor, lapse rate, surface albedo, and cloud feedback components) as diagnosed by Colman (2003a), Soden and Held (2006), and Winton (2006). The water vapor feedback constitutes by far the strongest feedback, with a multimodel mean and standard deviation of the feedback parameter [as estimated by Soden and Held (2006) for coupled GCMs participating in the IPCC Fourth Assessment Report (AR4) of the IPCC] of 1.80 ± 0.18 W m^{-2} K^{-1}, followed by the lapse rate feedback (-0.84 ± 0.26 W m^{-2} K^{-1}), the cloud feedback (0.69 ± 0.38 W m^{-2} K^{-1}), and the surface albedo feedback (0.26 ± 0.08 W m^{-2} K^{-1}). These results indicate that in GCMs, the water vapor feedback amplifies the earth's global mean temperature response (compared to a basic Planck response, see appendix A) by a

factor of 2 or more, the lapse rate feedback reduces it by about 20% (the combined water vapor plus lapse rate feedback amplifies it by 40%–50%),[2] the surface albedo feedback amplifies it by about 10%, and the cloud feedback amplifies it by 10%–50% depending on GCMs. Interestingly, these results do not substantially differ from those published in the pioneering work of Hansen et al. (1984).

Although the intermodel spread of feedback strength is substantial for all the feedbacks, it is the largest for cloud feedbacks. The comparison also reveals quite a large range in the strength of water vapor and lapse rate feedbacks among GCMs. A strong anticorrelation between the water vapor and lapse rate feedbacks of models is also seen, consistent with long-held views on the relationships between the two feedbacks (e.g., Cess 1975). A consequence of this anticorrelation is that the spread of the combined water vapor–lapse rate feedback is roughly half that of the individual water vapor or lapse rate feedbacks, smaller than that of cloud feedbacks, but slightly larger than that of the surface albedo feedback. As suggested by Colman (2003a), Soden and Held (2006), and Webb et al. (2005, manuscript submitted to *Climate Dyn.,* hereafter WEBB) the range of climate sensitivity estimates among models thus primarily results from the spread of cloud feedbacks, but also with a substantial contribution of the combined water vapor–lapse rate and surface albedo feedbacks. This spread in climate feedbacks and climate sensitivity is not a new issue. It is a long-standing problem that is central to discussions about the uncertainty of climate change projections. A number of reasons for the slow progress in this area are proposed.

First, climate feedback studies have long been focused on the derivation of global estimates of the feedbacks using diagnostic methods that are not directly applicable to observations and so do not allow any observational assessment (see Stephens 2005 for an extensive discussion of these aspects). Indeed, climate feedbacks are defined as partial derivatives [Eq. (A2)]. Although partial derivatives can be readily computed in models, it is not possible to compute them rigorously from observations because we cannot statistically manipulate the observations in such a way as to insure that only one variable is changing. Nevertheless, the derivation and the model-to-model comparison of feedbacks have played a key role in identifying the main sources of "uncertainties" (in the sense of intermodel differences) in climate sensitivity estimates.

Second, the evaluation of climate change feedbacks raises methodological difficulties because observed variations of the climate system may not be considered to be analogs of a global, long-term climate response to greenhouse gas forcing for example because (i) observed climate variations may not be in equilibrium with the forcing, (ii) the natural forcings associated with short-term insolation cycles (diurnal/seasonal) or with volcanic eruptions operate in the SW domain of the spectrum while long-term anthropogenic forcings associated with well-mixed greenhouse gases operate mostly in the LW domain, (iii) the geographical structures of natural and anthropogenic forcings differ, and (iv) the fluctuations in temperature and in large-scale atmospheric circulation at short and long time scales are not comparable. In addition, in nature multiple processes are usually operating to change climate, for instance volcanic eruptions, the El Niño–Southern Oscillation (ENSO), and the annual cycle are often present together, and attributing an observed change to a particular cause may be problematic. These limitations make relationships between temperature, water vapor, and clouds inferred from the current climate not directly useful to estimate feedback processes at work under climate change (Hartmann and Michelsen 1993; Bony et al. 1995; Lau et al. 1996).

Third, the complexity of the climate system and the innumerable factors potentially involved in the climate feedbacks have long been emphasized and considered as an obstacle to the assessment of feedbacks, both in nature and in models.

Given these difficulties, how may we evaluate the realism of the climate change feedbacks produced by GCMs and thereby reduce the uncertainty in climate sensitivity estimates? We think that a better appreciation of the *physical mechanisms behind the global estimates of climate feedbacks* would help us (i) to understand the reasons why climate feedbacks differ or not among models, (ii) to assess the reliability of the feedbacks produced by the different models, and (iii) to guide the development of strategies of model–data comparison relevant for observationally constraining some components of the global feedbacks.

With these issues in mind, we present below some simple conceptual frameworks that may help to guide our thinking, we review our current understanding of the main physical mechanisms involved in the different radiative feedbacks, and we discuss how observations may be used to constrain them in climate models. Although the cloud, water vapor, lapse rate, and ice feedbacks all interact with each other (in particular the cloud–surface albedo feedbacks in snow or sea ice regions, the water vapor–cloud feedbacks, and the water

---

[2] As explained by Hansen et al. (1984) and in appendix A, the feedback parameters and the feedback gains are additive but not the feedback factors.
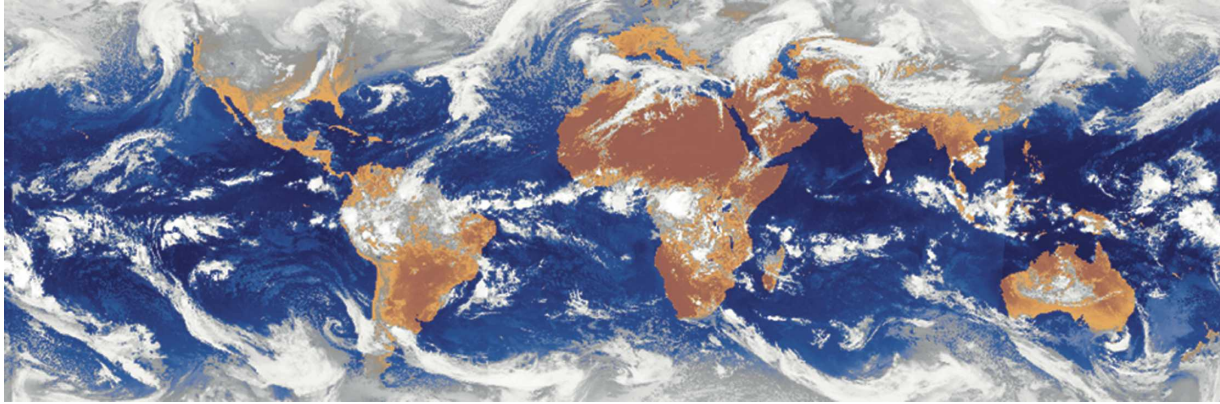
FIG. 2. Composite of instantaneous infrared imagery from geostationary satellites (at 1200 UTC 29 Mar 2004) showing the contrast between the large-scale organization of the atmosphere and of the cloudiness in the Tropics and in the extratropics. [From SATMOS (©METEO-FRANCE and Japan Meteorological Agency).]

vapor–lapse rate feedbacks), we will consider them separately for the sake of simplicity of presentation. Ordering the feedbacks according to their contribution to the spread of climate sensitivity estimates among GCMs (Fig. 1), we will consider in turn cloud feedbacks (section 2), the combined water vapor–lapse rate feedbacks (section 3), and cryosphere feedbacks (snow and sea ice, section 4). For this discussion, we will not attempt an exhaustive review of the literature, but will focus on major advances that have taken place since the TAR of the IPCC (Houghton et al. 2001).

2. Cloud feedbacks

Cloud feedbacks have long been identified as the largest internal source of uncertainty in climate change predictions, even without considering the interaction between clouds and aerosols[3] (Cess et al. 1990; Houghton et al. 2001). Recent comparisons of feedbacks produced by climate models under climate change show that the current generation of models still exhibits a large spread in cloud feedbacks, which is larger than for other feedbacks (Fig. 1). Moreover, for most models the climate sensitivity estimate still critically depends on the representation of clouds (e.g., Yao and Del Genio 2002; Ogura et al. 2005, manuscript submitted to *J. Meteor. Soc. Japan*). Defining strategies for evaluation of cloud feedback processes in climate models is thus of primary importance to better understand the range of model sensitivity estimates and to make climate predictions from models more reliable. Progress

has been made during the last few years in our understanding of processes involved in these feedbacks, and in the way these processes may be investigated in models and in observations.

a. Conceptual representations of the climate system

Much of our understanding of the climate system, and of climate feedbacks in particular, is due to studies using simple or conceptual models that capture the essential processes of the climate system in a simplified way (Pierrehumbert 1995; Miller 1997; Larson et al. 1999; Kelly et al. 1999; Lindzen et al. 2001; Kelly and Randall 2001). Drawing connections between simple climate model idealizations and the three-dimensional climate of nature or climate models would help to better understand and assess the climate feedbacks produced by complex models. As a first step toward that end, we present below some simple conceptual frameworks through which climate feedbacks and cloud feedbacks in particular may be analyzed. This will serve afterward as a pedagogical basis to synthesize results from recent observational, theoretical, and modeling studies.

As is already well known (and illustrated in Fig. 2), the atmospheric dynamics and thus the large-scale organization of the atmosphere is a strong function of latitude. In the Tropics, large-scale overturning circulations prevail. These are associated with narrow cloudy convective regions and widespread regions of sinking motion in the midtroposphere (generally associated with a free troposphere void of clouds and a cloud-free or cloudy planetary boundary layer). In the extratropics, the atmosphere is organized in large-scale baroclinic disturbances.

The large-scale circulation of the tropical atmosphere and its connection to cloudiness is shown as a schematic

---

[3] In this paper, we will not discuss the microphysical feedbacks associated with the interaction between aerosols and clouds. As Lohmann and Feichter (2005) say: "The cloud feedback problem has to be solved in order to assess the aerosol indirect forcing more reliably."
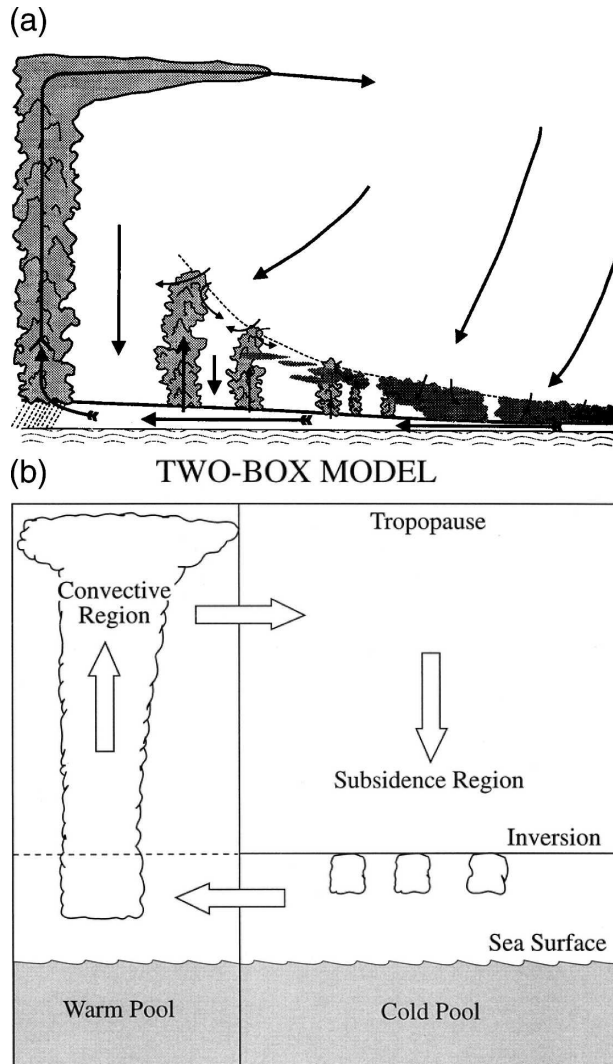
(a)

(b)

TWO-BOX MODEL

FIG. 3. Two conceptual representations of the relationship between cloudiness and large-scale atmospheric circulation in the Tropics: (a) structure of the tropical atmosphere, showing the various regimes, approximately as a function of SST (decreasing from left to right) or mean large-scale vertical velocity in the midtroposphere (from mean ascending motions on the left to large-scale sinking motions on the right). [From Emanuel (1994).] (b) Two-box model of the Tropics used by Larson et al. (1999). The warm pool has high convective clouds and the cold pool has boundary layer clouds. Air is rising in the warm pool and sinking across the inversion in the cold pool.

scale circulation and by the constraint of having a weak temperature gradient in the free troposphere.

A more continuous idealization of the tropical circulation was proposed by Bony et al. (2004). This uses the 500-hPa large-scale vertical velocity ω as a proxy for large-scale vertical motions of the atmosphere and decomposes the Hadley–Walker circulation as a series of dynamical regimes defined using ω. In the Tropics, nearly all of the upward motion associated with ensemble-average ascent occurs within cumulus clouds, and gentle subsidence occurs in between clouds. Since the rate of subsidence in between clouds is strongly constrained by the clear-sky radiative cooling and thus nearly invariant, an increase of the large-scale mean ascent corresponds, to first order, to an increase of the mass flux in cumulus clouds (Emanuel et al. 1994). Therefore, considering dynamical regimes defined from ω allows us to classify the tropical regions according to their convective activity, and to segregate in particular regimes of deep convection from regimes of shallow convection. The statistical weight of the different circulation regimes (Fig. 4) emphasizes the large portion of the Tropics associated with moderate sinking motions in the midtroposphere (such as found over the trade wind regions), and the comparatively smaller weight of extreme circulation regimes associated with the warm pool or with the regions of strongest sinking motion and static stability such as found at the eastern side of the ocean basins. These extreme regimes correspond to the tails of the ω probability distribution function. The atmospheric vertical structure (observed or modeled) can then be composited within each dynamical regime. Illustrations of the dependence of cloud radiative properties and of precipitation on the large-scale circulation are displayed in Figs. 4b,c, showing the satellite-derived precipitation and cloud radiative forcing (CRF) as a function of ω (ω being derived from meteorological reanalyses). These increase as the vigor of the convective mass flux increases.

At midlatitudes, the atmosphere is mostly organized in synoptic weather systems (Fig. 2). An idealized baroclinic disturbance is represented in Fig. 5a, showing the warm and cold fronts outward from the low-level pressure center of the disturbance, together with the occurrence of sinking motion behind the cold front and rising motion ahead of the warm front. As discussed in Wallace and Hobbs (1977), the different parts of the system are associated with specific cloud types, ranging from thin low-level cumulus clouds behind the cold front, thin upper-level clouds ahead of the warm front, and thick precipitating clouds over the fronts (Fig. 5b).

Given the strong connection between the large-scale atmospheric circulation and the distribution of water
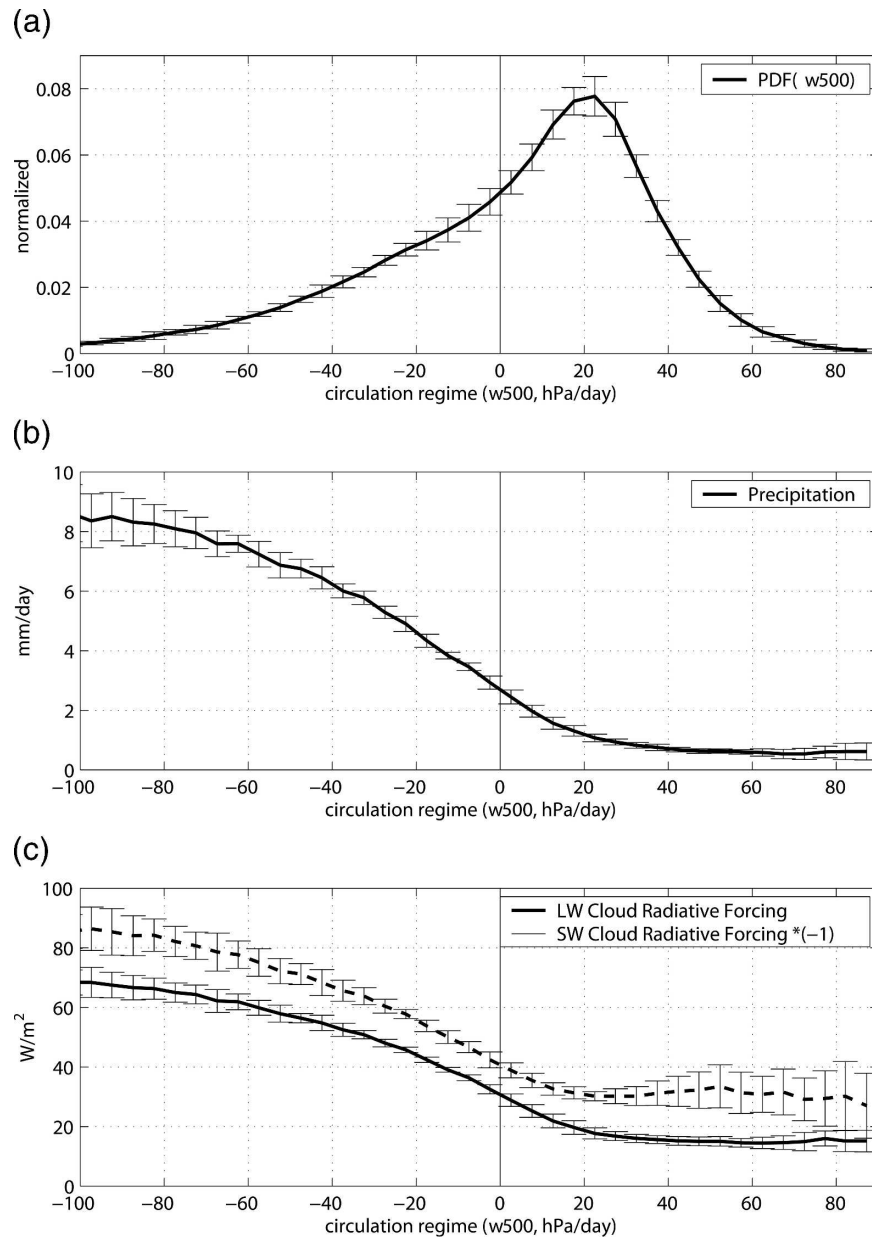
in Fig. 3a. In idealized box models such as those developed by Pierrehumbert (1995) or Larson et al. (1999), the circulation is idealized even further by partitioning the Tropics into a single moist, precipitating area covered by convective clouds and a single dry, nonprecipitating area associated with sinking motion in the midtroposphere and a clear-free or cloudy boundary layer (Fig. 3b). These areas are coupled by the large-

FIG. 4. (a) PDF P_ω of the 500-hPa monthly mean large-scale vertical velocity ω_{500} in the Tropics (30°S–30°N) derived from ERA-40 meteorological reanalyses, and composite of the monthly mean (b) GPCP precipitation and (c) ERBE-derived longwave and shortwave (multiplied by −1) cloud radiative forcing in different circulation regimes defined from ERA-40 ω_{500} over 1985–89. Vertical bars show the seasonal standard deviation within each regime. [After Bony et al. (2004).]

vapor and clouds, understanding cloud (and water vapor) feedbacks under climate change requires the examination of at least two main issues: 1) how might the large-scale circulation change under global warming and how might that affect the global mean radiation budget (even without any specific change in the atmospheric properties under given dynamic conditions), and 2) how might the global climate warming affect the water vapor and cloud distributions under specified dynamic conditions.

b. Our understanding of cloud feedback processes

1) DYNAMIC AND THERMODYNAMIC INFLUENCES

The Tropics and the extratropics are associated with a large spectrum of cloud types, ranging from low-level
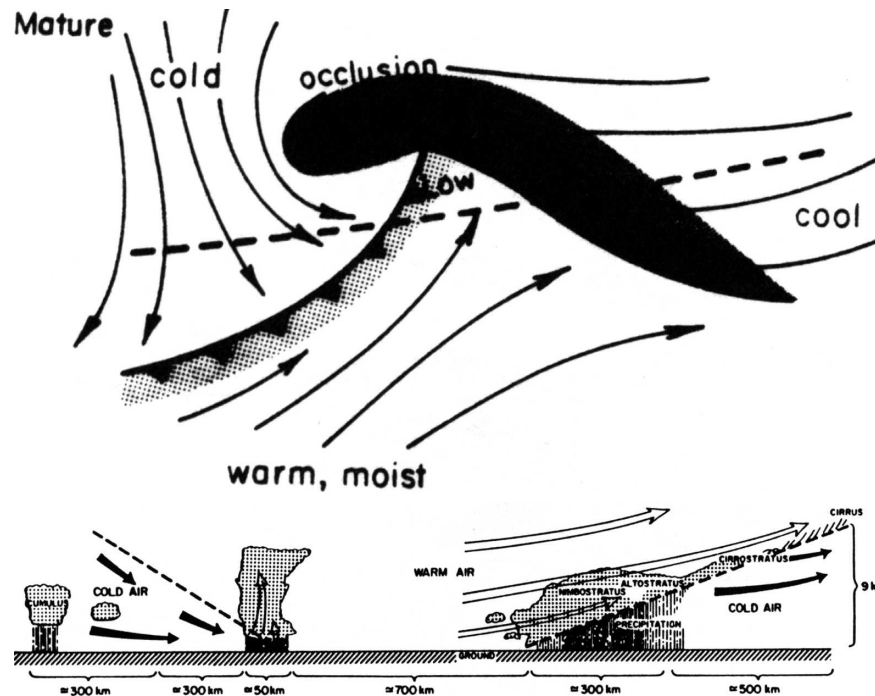
FIG. 5. (top) Schematic of a mature extratropical cyclone represented in the horizontal plane. Shaded areas are regions of precipitation. [From Cotton (1990).] (bottom) Schematic vertical cross section through an extratropical cyclone along the dashed line reported in the top showing typical cloud types and precipitation. [From Cotton (1990), after Houze and Hobbs (1982).]

boundary layer clouds to deep convective clouds and anvils. Because of their different top altitudes and optical properties, the different cloud types affect the earth's radiation budget in various ways. Understanding cloud radiative feedbacks requires an understanding of how a change in climate may affect the distribution of the different cloud types and their radiative properties, and an estimate of the impact of such changes on the earth's radiation budget. As discussed in section 2a, the occurrence of the cloud types is controlled partly by the large-scale atmospheric circulation (Figs. 3 and 5), and by many other factors such as surface boundary conditions, boundary layer stratification, wind shear, etc. By making the background relationship between cloud properties and large-scale circulation more explicit, one may more easily isolate other influences (e.g., the impact of a change in surface temperature or in the thermodynamic structure of the troposphere). Similarly, one may analyze the cloud response to a climate change by considering on one hand the part of cloud changes that may be simply explained by changes in the large-scale flow, and on the other the part that may be explained by other factors, such as an intrinsic dependence of cloud properties on temperature (section 2a).

In the Tropics, the dynamics are known to control to a large extent changes in cloudiness and cloud radiative forcing at the regional scale (Hartmann and Michelsen 1993; Bony et al. 1997; Chen et al. 2002; Williams et al. 2003; Bony et al. 2004). Regional circulation changes are often associated with spatial shifts of large-scale dynamical features, and therefore compensations can occur when considering a wider domain. At the Tropicswide scale, a change in circulation may change the tropically averaged cloud radiative forcing and radiation budget (even in the absence of any change in cloud properties) if circulation changes are associated not only with a spatial redistribution of convective and subsidence regions, but also with a global strengthening or a weakening of the Hadley–Walker circulation. Simple box models such as that illustrated in Fig. 3b show that a change in the large-scale atmospheric circulation can be associated with a change in the ratio of moist convective and dry subsidence areas of the Tropics (e.g., Larson et al. 1999). As Pierrehumbert (1995) and Lindzen et al. (2001) pointed out, a change in that ratio constitutes an efficient way to modify the longwave cooling to space and thereby affect the surface temperature change induced by an external perturbation.

A strengthening of the Hadley–Walker circulation over the last decade has been seen in observations and meteorological analyses (Chen et al. 2002; Mitas and Clement 2005). But Clement and Soden (2005) showed

that the tropical-mean radiation budget was remarkably insensitive to similar changes in the circulation. In a warmer global climate, simple climate models, cloud-resolving models (CRMs), mesoscale models, and GCMs all suggest that the strength of the tropical circulation could change (Miller 1997; Kelly and Randall 2001; Larson and Hartmann 2003; Bony et al. 2004; Peters and Bretherton 2005). However, Bony et al. (2004) and Wyant et al. (2006, hereafter WYANT) found that tropical circulation changes occurring in idealized climate warming experiments did not greatly affect the tropically averaged radiation budget. Therefore, these studies suggest that as a first step, changes in the tropical mean radiation budget or cloud radiative forcing may be understood by focusing on processes that affect clouds and radiation under specified dynamical conditions.

At midlatitudes, the potential for a change in the baroclinicity of the atmosphere and consequently in the storm tracks is also present. Observational studies at the decadal time scale indicate that changes in the distribution and in the strength of baroclinic eddies can actually occur (McCabe et al. 2001; Paciorek et al. 2002; Fyfe 2003). In a warming climate, the potential for such changes is also present, owing to the effect of changing meridional temperature gradients and land–sea temperature contrasts and of increasing water vapor in the atmosphere (Held 1993; Lapeyre and Held 2004). Indeed (as illustrated in Fig. 7), several climate models report a decrease in overall storm frequency and increases in storm intensity in increased CO_2 climate conditions (Lambert 1995; Katzfey and Mcinnes 1996; Carnell and Senior 1998; Sinclair and Watterson 1999; Tselioudis et al. 2000; Geng and Sugi 2003). As will be discussed below, several recent studies have used observations to investigate how a change in the dynamics of midlatitudes could affect the cloud radiative forcing and constitute a component of cloud feedback under climate change (Tselioudis and Rossow 2006, hereafter TR; Norris and Iacobellis 2005). Other studies investigate how a change in temperature under given dynamical conditions could affect cloud properties and/or the cloud radiative forcing (Del Genio and Wolf 2000; Norris and Iacobellis 2005). The relative importance under climate change of these two components of midlatitude cloud feedbacks in GCMs is currently unknown.

In the following, we discuss feedback processes that may be associated with tropical deep convective and boundary layer clouds, extratropical cloud systems, and polar clouds.

2) Deep convective clouds

Several climate feedback mechanisms involving convective clouds have been examined with observations and simple climate models, and also increasingly with CRMs.

A surprising property of clouds observed in tropical oceanic deep convective regimes is that their LW and SW CRF nearly cancel each other out (Ramanathan et al. 1989). Kiehl (1994) argued this is coincidental, while Hartmann et al. (2001) suggest this is a property of the *ensemble* of cloud types that occurs in association with deep convection in the Tropics. Hartmann et al. (2001) argue that this ensemble of clouds adjusts through dynamical feedbacks in the ocean–atmosphere system so as to keep the radiation budget of convective regions close to that of adjacent nonconvective regions. Neither coupled GCM (e.g., Kiehl and Gent 2004) nor CRM (e.g., Wu et al. 1999) simulations show evidence that the observed cancellation is a universal feature of tropical climate. Note however that given uncertainties in the representation of cloud radiative properties by GCMs and CRMs, this may not be a definitive result.

Analyzing geostationary data over the western tropical Pacific, Lindzen et al. (2001) hypothesized that a warming climate might lead to decreased anvil cloud fraction owing to an increase with temperature of the precipitation efficiency of cumulonimbus clouds and decreased water detrained in the upper troposphere (the so-called iris hypothesis). However, doubts about the evidence provided so far have been expressed by several studies and this has been a polemical issue (Chambers et al. 2002; Del Genio and Kovari 2002; Fu et al. 2002; Hartmann and Michelsen 2002; Lin et al. 2002, 2004; Lindzen et al. 2002). Nevertheless, the potential impact of an intrinsic temperature dependence of deep convective clouds microphysics on climate sensitivity remains an open issue.

Hartmann and Larson (2002) proposed that the emission temperature of tropical anvil clouds is essentially independent of the surface temperature, and that it will thus remain unchanged during climate change [the so-called fixed anvil temperature (FAT) hypothesis]. Their reasoning, tested with a mesoscale model, is that the altitude of convective detrainment occurs where the clear-sky longwave radiative cooling rapidly declines with height, and that the temperature at which this decline occurs is constrained by the dependence of water vapor emission on temperature. Their hypothesis is consistent with CRM simulations (Bretherton et al. 2006, showing that in a warmer climate, the vertical profiles of mid- and upper-tropospheric cloud fraction, condensate, and relative humidity all tend to be displaced upward in height in lockstep with the temperature. This vertical displacement is found also in CRM simulations of Tompkins and Craig (1999); however, these show a slight increase of the cloud-top tempera-

ture with increasing surface temperature. Comparable simulations with other CRMs are thus needed to establish the robustness of these results, as well as its investigation in climate models.

3) LOW-LATITUDE BOUNDARY LAYER CLOUDS

Boundary layer clouds have a strongly negative CRF (Harrison et al. 1990; Hartmann et al. 1992) and cover a very large fraction of the area of the Tropics (e.g., Norris 1998b). Understanding how they may change in a perturbed climate therefore constitutes a vital part of the cloud feedback problem. Unfortunately, our understanding of the physical processes that control boundary layer clouds and their radiative properties is currently very limited.

It has been argued based on the Clausius–Clapeyron formula that in a warmer climate, water clouds of a given thickness would hold more water and have a higher albedo (Somerville and Remer 1984; Betts and Harshvardhan 1987). But the analysis of satellite observations show evidence of decreasing cloud optical depth and liquid water path with temperature in low-latitude boundary layer clouds (Tselioudis and Rossow 1994; Greenwald et al. 1995; Bony et al. 1997). This may be due to the confounding effect of many physical processes, such as increases with temperature in precipitation efficiency or decreases with temperature in cloud physical extent (Tselioudis et al. 1998; Del Genio and Wolf 2000).

Klein and Hartmann (1993) showed an empirical correlation between mean boundary layer cloud cover and lower-tropospheric stability (defined in their study as the difference of 700-hPa and near-surface potential temperature). When imposed in simple two-box models of the tropical climate (Miller 1997; Clement and Seager 1999; Larson et al. 1999) or into some GCMs' parameterizations of boundary layer cloud amount [e.g., in the National Center for Atmospheric Research (NCAR) Community Climate System Model verion 3 (CCSM3)], this empirical correlation leads to a substantial increase in low cloud cover in a warmer climate driven by the larger stratification of warmer moist adiabats across the Tropics, and produces a strong negative feedback. However variants of lower-tropospheric stability that may predict boundary layer cloud cover just as well as the Klein and Hartmann (1993) parameterization, would not necessarily predict an increase in boundary layer cloud in a warmer climate (e.g., Williams et al. 2006; Wood and Bretherton 2006).

The boundary layer cloud amount is strongly related to the cloud types present, which depend on many synoptic- and planetary-scale factors (Klein 1997; Norris 1998a; Norris and Klein 2000). Factors such as changes in the vigor of shallow convection, possible precipitation processes, and changes in capping inversion height and cloud thickness can outweigh the effect of static stability. These factors depend on local physical processes but also on remote influences, such as the effect of changing deep convective activity on the free tropospheric humidity of subsidence regions (Miller 1997; Larson et al. 1999; Kelly and Randall 2001). Evidence from observations, large-eddy simulation models, or climate models for the role of these different factors in cloud feedbacks is currently very limited.

4) EXTRATROPICAL CLOUD SYSTEMS

In the midlatitude regions of both hemispheres, clouds are closely controlled by the large-scale atmospheric dynamics (Fig. 5). Lau and Crane (1995, 1997), and more recently Norris and Iacobellis (2005) illustrate this nicely by using meteorological analyses and satellite or surface cloud observations: extratropical cyclones in the storm tracks generate thick, high-top frontal clouds in regions of synoptic ascent and low-level clouds (of cumulus, stratocumulus or stratus type depending on the boundary layer stratification) under synoptic descent (Fig. 6).

Several studies have applied statistical compositing techniques to cloud, radiation, and atmospheric dynamics datasets in order to examine variations of cloud and radiation properties with dynamical parameters like sea level pressure and midtropospheric vertical velocity. Weaver and Ramanathan (1996) showed that in the summertime North Pacific shortwave cloud forcing associated with midlatitude cyclones is about -150 W m^{-2} compared to a forcing of about -80 W m^{-2} for subtropical stratocumulus decks. Tselioudis et al. (2000) found that differences in shortwave fluxes between low and high pressure regimes in the northern midlatitudes range seasonally between -5 and -50 W m^{-2}, while differences in longwave fluxes range between 5 and 35 W m^{-2}. The net flux differences between the two regimes introduce a wintertime warming in the low versus the high pressure regimes of 5–15 W m^{-2} and a cooling in all other seasons of 10–40 W m^{-2}. Norris and Weaver (2001) found cloud radiative forcing differences of about 50 W m^{-2} between large-scale ascent and subsidence regions in the summertime North Atlantic storm track.

Using current climate observations to composite radiation properties of shallow, medium, and deep baroclinic storms, TR estimate the effect that model-predicted storm frequency decreases and storm strength increases with climate warming (Carnell and Senior 1998; Fig. 7 of this paper) would have on the northern midlatitude radiation budget. They find that
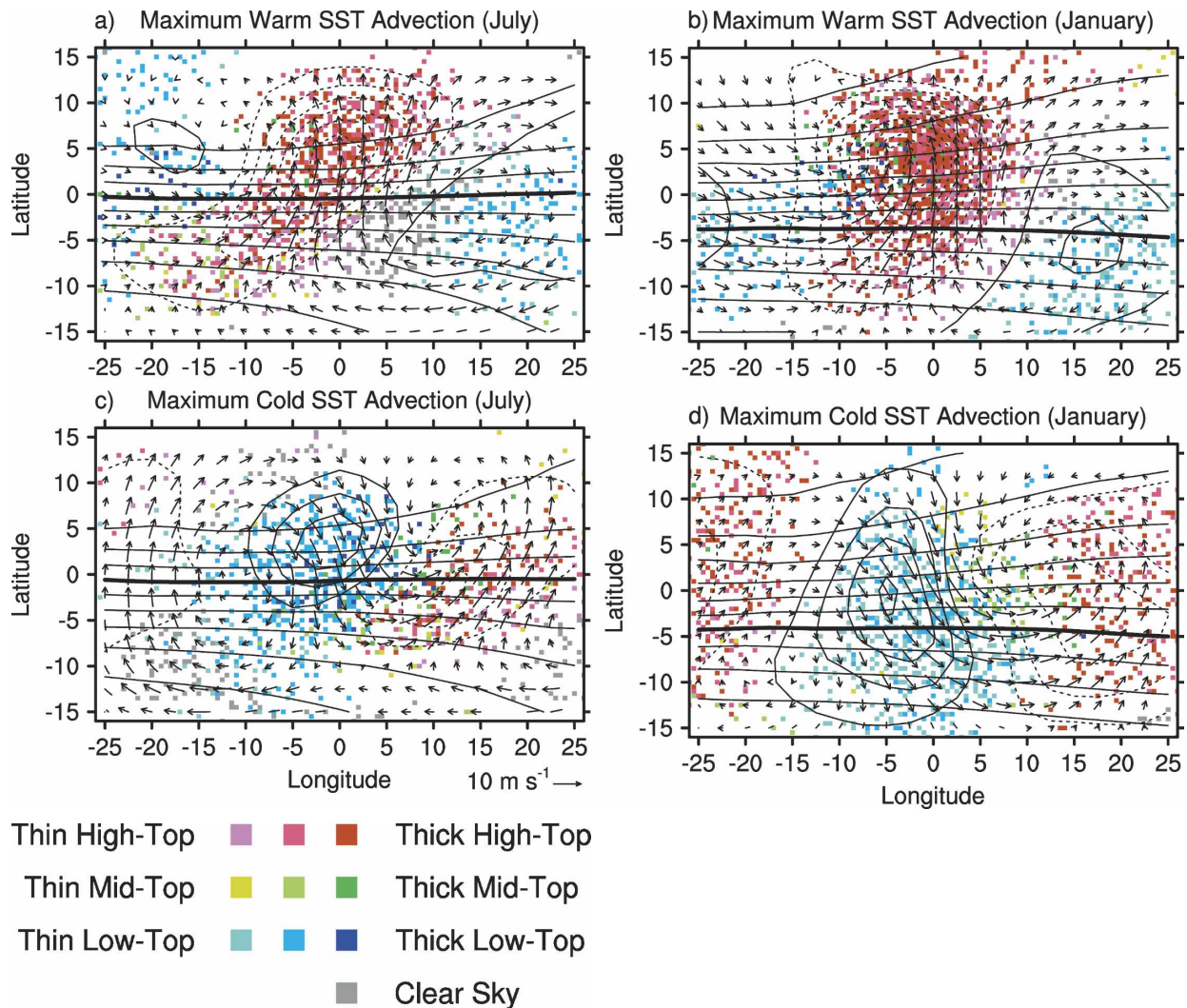
FIG. 6. Composite spatial distributions of 1000-hPa wind (arrows), SST (nearly horizontal lines), 500-hPa pressure vertical velocity (other solid and dashed lines), and ISCCP cloud anomalies (color) centered on locations within the region 30°–50°N, 155°–215°E where advection of the 1000-hPa wind over the SST gradient ($-\mathbf{V} \cdot \nabla \mathbf{SST}$) is (a) maximum positive during July, (b) maximum positive during January, (c) maximum negative during July, and (d) maximum negative during January. Composites were constructed from local noon data during 1984–2001. The SST contour interval is 2°C with a thick line for the 16°C isotherm. The vertical velocity contour interval is 20 hPa day^{-1} for July and 40 hPa day^{-1} for January with negative (upward) contours dashed, positive (downward) contours solid, and no zero contour. Each 2.5° × 2.5° grid box in the plot is filled with 25 pixels, and each pixel represents an additional 2% cloud amount or clear-sky frequency beyond the climatological value for the ISCCP category associated with that color (see legend in figure). Only cloud anomalies statistically significant at 95% are shown, and negative cloud anomalies are not plotted. [From Norris and Iacobellis (2005).]

while the decrease in storm frequency would produce shortwave warming and longwave cooling, the increase in storm strength would produce changes of the opposite sign, and that when the two storm changes are taken together the increase in storm strength dominates producing a shortwave cooling effect of $0-3.5$ W m^{-2} and a longwave warming effect of $0.1-2.2$ W m^{-2}. Examining cloud observations and reanalysis dynamical parameters, Norris and Iacobellis (2005) suggest that a decrease in the variance of vertical velocity would lead

to a small decrease in mean cloud optical thickness and cloud-top height.

Several studies have also investigated the dependence of extratropical cloud properties on temperature. For instance, Del Genio and Wolf (2000) show that for low-level continental clouds, the liquid water content shows no detectable temperature dependence while the physical thickness decreases with temperature, resulting in a decrease of the cloud water path and optical thickness as temperature rises. Examining extratropical
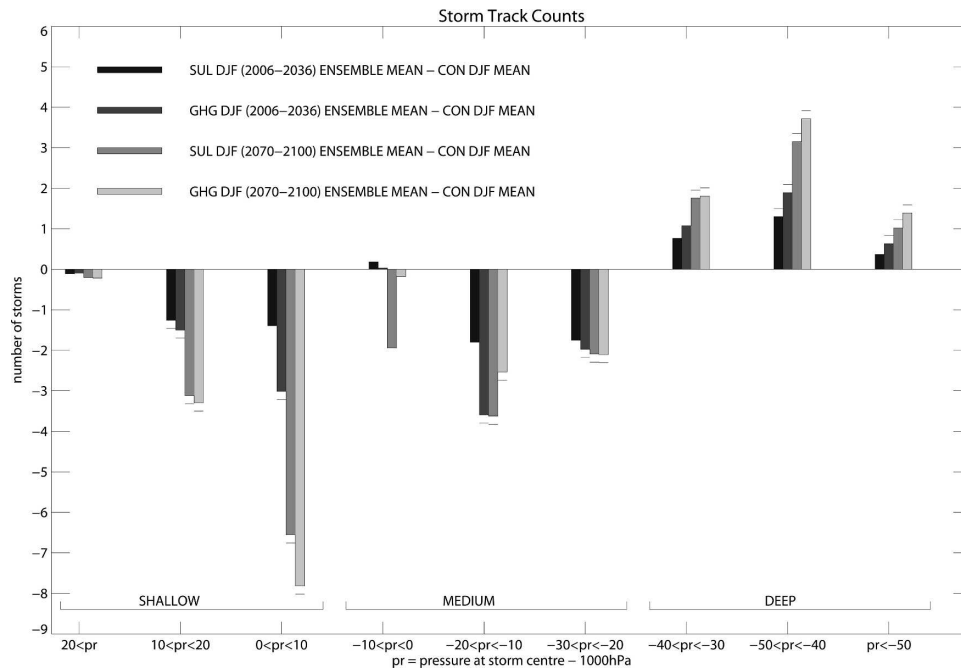
FIG. 7. Number of storm tracks per 90-day December–January–February season in each central pressure band (pr, pressure at storm center − 1000 hPa). Dark, medium dark, medium light, and light shadings (first, second, third, and fourth peak from left of each group) show the change in the number of storms (relative to the control experiment) in the experiment forced by both greenhouse gases and the direct effect of aerosols (SUL) or by only greenhouse gases (GHG) for two different time periods. Horizontal bars at the end of peaks show changes that are significant at the 1% level. [From Carnell and Senior (1998).]

clouds over the North Pacific, Norris and Iacobellis (2005) suggest that a uniform surface warming would result in decreased cloud amount and optical thickness over a large range of dynamical conditions, producing a decrease of the reflection of solar radiation back to space and hence contributing to a positive radiative feedback (Fig. 8).

These few studies suggest that the change in midlatitude clouds under climate change may generate a positive feedback. However, other factors not considered in these studies may play also an important role. In particular, climate change is likely to be associated with a latitudinal shift of the storm tracks (e.g., Hall et al. 1994; Yin 2005); owing to the strong dependence of the SW CRF on insolation, this dynamical shift may also change the cloud radiative forcing by a few watts per meter squared. Therefore, it is still unknown whether the combined effects of dynamical and temperature changes would still be associated with a positive feedback under a climate change. In any event, since in midlatitudes the poleward heat transport of the ocean–atmosphere system is largely due to the atmospheric eddies that make up the storm tracks, and since the heat transport is affected by cloud radiative effects (Zhang and Rossow 1997), extratropical storms, cloud radiative effects, and the poleward heat transport are all coupled. Weaver (2003) argues that this coupling constitutes a feedback process potentially important for the climate system.

5) POLAR CLOUDS

The role of polar cloud feedbacks in climate sensitivity has been emphasized during the last few years (Holland and Bitz 2003; Vavrus 2004), polar regions being the most sensitive regions of the earth and clouds exerting a large influence on the surface radiation budget of these regions (Curry et al. 1996). A comparison of models (Holland and Bitz 2003) shows a positive correlation between the simulated polar amplification and the increase in polar cloud cover (especially during winter), which suggests a positive polar cloud feedback owing to the local effect of clouds on the downward surface longwave radiation. This is also suggested by Vavrus (2004) who diagnosed a positive cloud feedback in his model accounting for approximately one-third of the global warming and 40% of the Arctic warming. However, he pointed out the nearly equal impact of local increase and remote decrease (at low and midlatitudes) of cloudiness in the enhanced Arctic warming.
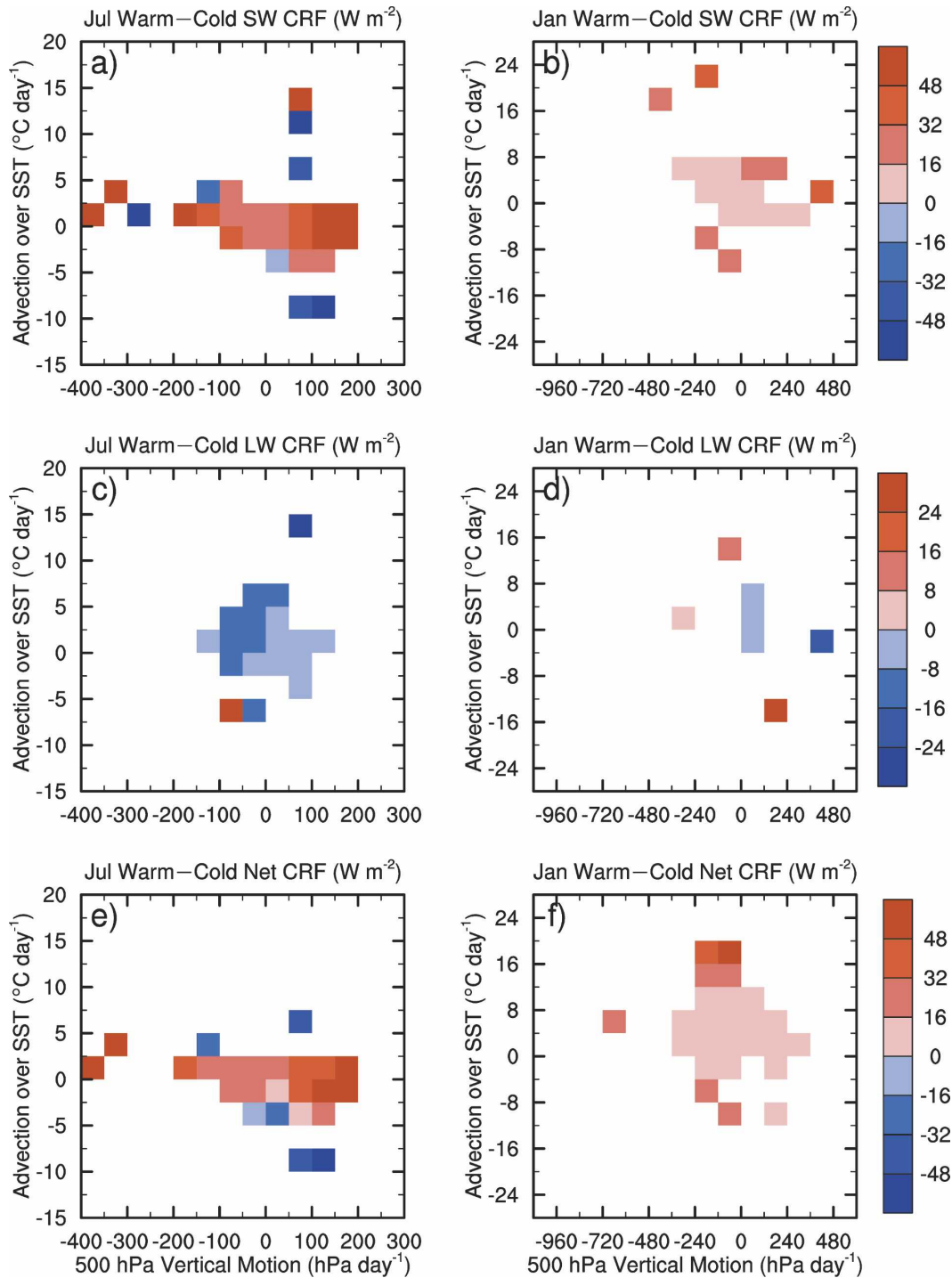
FIG. 8. Composites of the ERBE (a), (b) SW, (c), (d) LW, (e), (f) and NET cloud radiative forcing difference between the upper (warm) and lower (cold) SST terciles for July and January during 1985–89 in ω_{500} and advection intervals over the North Pacific (25°–55°N, 145°–225°E). The magnitude of SW CRF decrease with rising temperature under most conditions of vertical velocity and SST advection (the advection of the 1000-hPa wind over the SST gradient). The cloud amount and optical thickness also decrease with rising temperature (not shown). The magnitude of LW CRF decreases, but the change in SW CRF is larger, so net CRF becomes less negative (or more positive) with warmer temperature. [From Norris and Iacobellis (2005).]

c. Cloud changes simulated by models under global warming

Several multimodel analyses of cloud feedbacks produced by GCMs under sea surface temperature (SST) or CO_2 perturbation have been carried out since the TAR under the auspices of the Coupled Model Intercomparison Project (CMIP; Meehl et al. 2000), the Cloud Feedback Intercomparison Project (CFMIP; McAvaney and Le Treut 2003), or the Low-Latitude Cloud Feedbacks Climate Process Team project (CPT; Bretherton et al. 2004). These analyses show no consensus in the global response of clouds and cloud radiative forcing to a given climate perturbation. Diagnosing cloud feedbacks through the partial radiative perturbation (PRP) method (appendix B) or a variant of it, Colman (2003a) and Soden and Held (2006) suggest that the global cloud feedback is positive in all the models, but exhibit large intermodel differences in the magnitude of this feedback. Roughly half of the models exhibit a negative anomaly of the global net CRF in response to global warming and half exhibit a positive anomaly (Soden and Held 2006; WEBB). This apparent discrepancy between the sign of cloud feedbacks estimated from the PRP method and the sign of global CRF anomalies arises from the impact on CRF changes of the interaction between water vapor and surface albedo changes with cloud changes (Zhang et al. 1994; Soden et al. 2004, WEBB, see also appendix B). For instance, WEBB show that changes in the shortwave CRF, which are collocated with changes in surface albedo at mid- and high latitudes have a substantial effect on global CRF changes. However, the cloud feedback estimates diagnosed from either method are well correlated, and they exhibit a large and similar range of magnitude among GCMs (Soden and Held 2006).

Where does the spread of global cloud feedback estimates come from? The frequencies of occurrence of different cloud types (both observed and modeled) are highly unequal (e.g., Zhang et al. 2005), and so the behavior of certain clouds may matter more than that of others in explaining the range of cloud feedbacks among models. Several studies—Williams et al. (2003, 2006), Bony et al. (2004), and WYANT —show that the responses of deep convective clouds and of low-level clouds differ among GCMs. Changes in the water content of the different types of clouds also differ strongly among GCMs (WYANT). The analysis and the comparison of cloud feedbacks in the nine CFMIP slab model CO_2-doubling experiments (WEBB) shows that differences in cloud feedbacks in areas dominated by low-top cloud responses make the largest contribution to the variance in the global feedback. Studies with
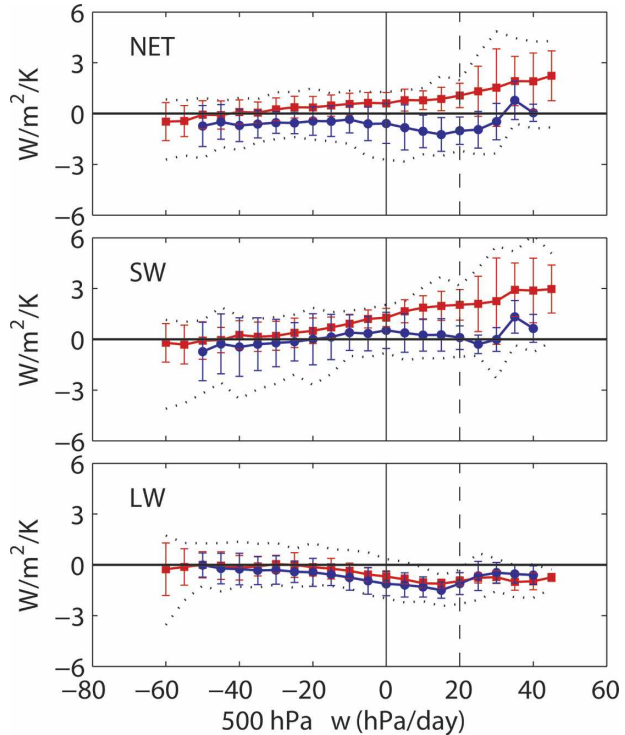

FIG. 9. Sensitivity (in W m^{-2} K^{-1}) of the tropical (30°S–30°N) NET, SW, and LW CRF to SST changes associated with climate change (in a scenario in which the CO_2 increases by 1% yr^{-1}) derived from 15 coupled ocean–atmosphere GCMs participating in the AR4. The sensitivity is computed for different regimes of the large-scale atmospheric circulation (the 500-hPa large-scale vertical pressure velocity is used as a proxy for large-scale motions, negative values corresponding to large-scale ascent and positive values to large-scale subsidence). Results are presented for two groups of GCMs: models that predict a positive anomaly of the tropically averaged NET CRF in climate change (in red, eight models) and models that predict a negative anomaly (in blue, seven models). [From Bony and Dufresne (2005).]

slightly older coupled model versions (Volodin 2004; Stowasser et al. 2006) also suggest that low cloud responses are responsible for differences in global climate sensitivity. The comparison of cloud feedbacks in 15 of the AR4 coupled ocean–atmosphere GCMs (Bony and Dufresne 2005) shows that, in the tropical region, the CRF response differs most between models in subsidence regimes, which also suggests a dominant role for low-level clouds in the diversity of tropical cloud feedbacks (Fig. 9). As discussed in Bony et al. (2004), this is due both to differing predictions from GCMs of the response of clouds in these regimes (Fig. 9), and to the large fraction of the earth covered by these regimes (Fig. 4a). Figure 10 suggests that in the AR4 slab model CO_2-doubling experiments, the spread in tropical cloud feedbacks is substantial both in the Tropics and in the extratropics, and tends to be larger in the Tropics.
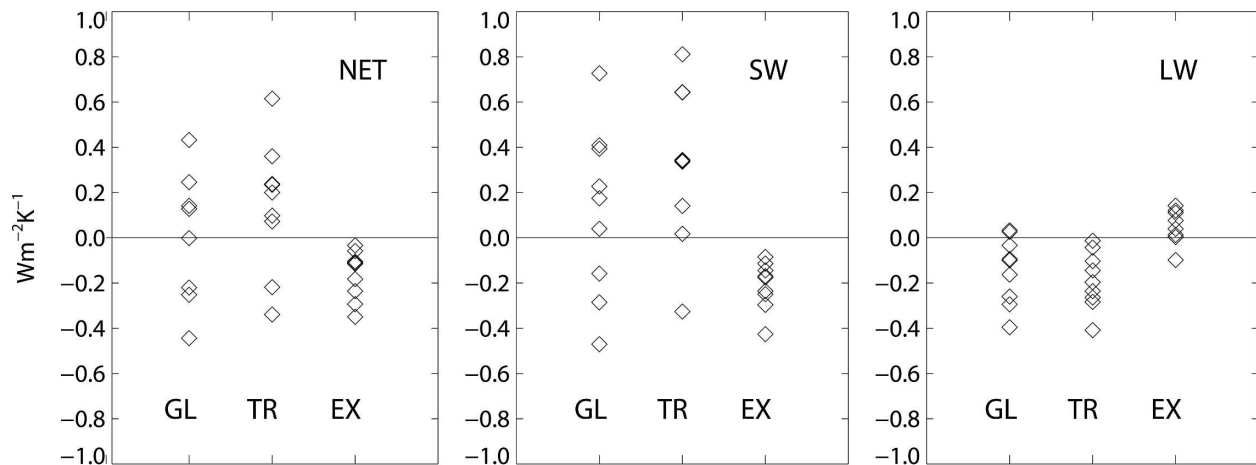
FIG. 10. Global change in the (left) NET, (middle) SW, and (right) LW CRF normalized by the change in global mean surface air temperature predicted by AR4 mixed layer ocean atmosphere models in 2xCO₂ equilibrium experiments. For each panel, results (in W m⁻² K⁻¹) are shown for global (GL), tropical (TR, 30°S–30°N) and extratropical (EX) areas. The intermodel spread of the global CRF response to climate warming primarily arises from different model predictions of the change in tropical SW CRF. (Adapted from WEBB.)

d. New approaches for evaluating clouds in climate models

The evaluation of clouds in climate models has long been based on comparisons of observed and simulated climatologies of the total cloud amount and radiative fluxes at the top of the atmosphere. Such comparisons do not offer stringent constraints on cloud radiative feedbacks produced by models under climate change. In that regard, three main advances have been made over the last few years.

First, comparisons between the observed and simulated cloud fields are increasingly done by applying an "ISCCP [International Satellite Cloud Climatology Project] simulator" (Rossow and Schiffer 1999) to the models to produce cloud diagnostics stratified into cloud-top altitude ranges and optical properties directly comparable to satellite retrievals (Yu et al. 1996; Klein and Jakob 1999; Webb et al. 2001; Lin and Zhang 2004; Zhang et al. 2005; WYANT). This makes it possible to evaluate the cloudiness in terms of cloud types and cloud properties, making it harder for models to get agreement with the observed radiative fluxes through compensating errors, as demonstrated in Webb et al. (2001).

Second, efforts have been put into evaluating the ability of climate models to reproduce cloud variations observed at the diurnal (Yang and Slingo 2001; Dai and Trenberth 2004; Slingo et al. 2004; Tian et al. 2004), seasonal (Tsushima and Manabe 2001; Zhang et al. 2005), interannual (Potter and Cess 2004; Ringer and Allan 2004) and decadal (Wielicki et al. 2002; Allan and Slingo 2002) time scales. Emphasis has been put in particular on inaccuracies in the models' simulation of the

amplitude and/or the phase of the diurnal cycle of the cloudiness, and in reproducing the decadal variations of the radiation budget shown by observations in the Tropics.

Third, a new class of diagnostic tests has been developed, including compositing and clustering techniques, which are more closely related to our understanding of cloud feedback mechanisms and are therefore more relevant for the interpretation and the evaluation of the models' cloud feedbacks than traditional model–data comparisons. In that vein, relationships between cloud properties and large-scale dynamics at midlatitudes have been examined (Lau and Crane 1995, 1997; Tselioudis et al. 2000; Norris and Weaver 2001; Jakob and Tselioudis 2003; TR; Lin and Zhang 2004; Norris and Iacobellis 2005), and the relationships between tropical clouds and sea surface temperature have been investigated within particular dynamical regimes (Bony et al. 1997; Williams et al. 2003; Bony et al. 2004; Ringer and Allan 2004; Bony and Dufresne 2005; WYANT).

1) COMPOSITING OR CLUSTERING APPROACHES

The ability of climate model simulations to reproduce relationships between clouds, radiation, and dynamics was examined by applying the same statistical compositing techniques to model simulations as to observations, and by applying satellite data simulators to models. Several studies have reported biases in the simulation of the cloud radiative forcing by the generation of climate models used in the TAR of the IPCC (Norris and Weaver 2001; Webb et al. 2001; Williams et al. 2003; Bony et al. 2004; Potter and Cess 2004; Ringer and Allan 2004). This revealed biases in the simulation
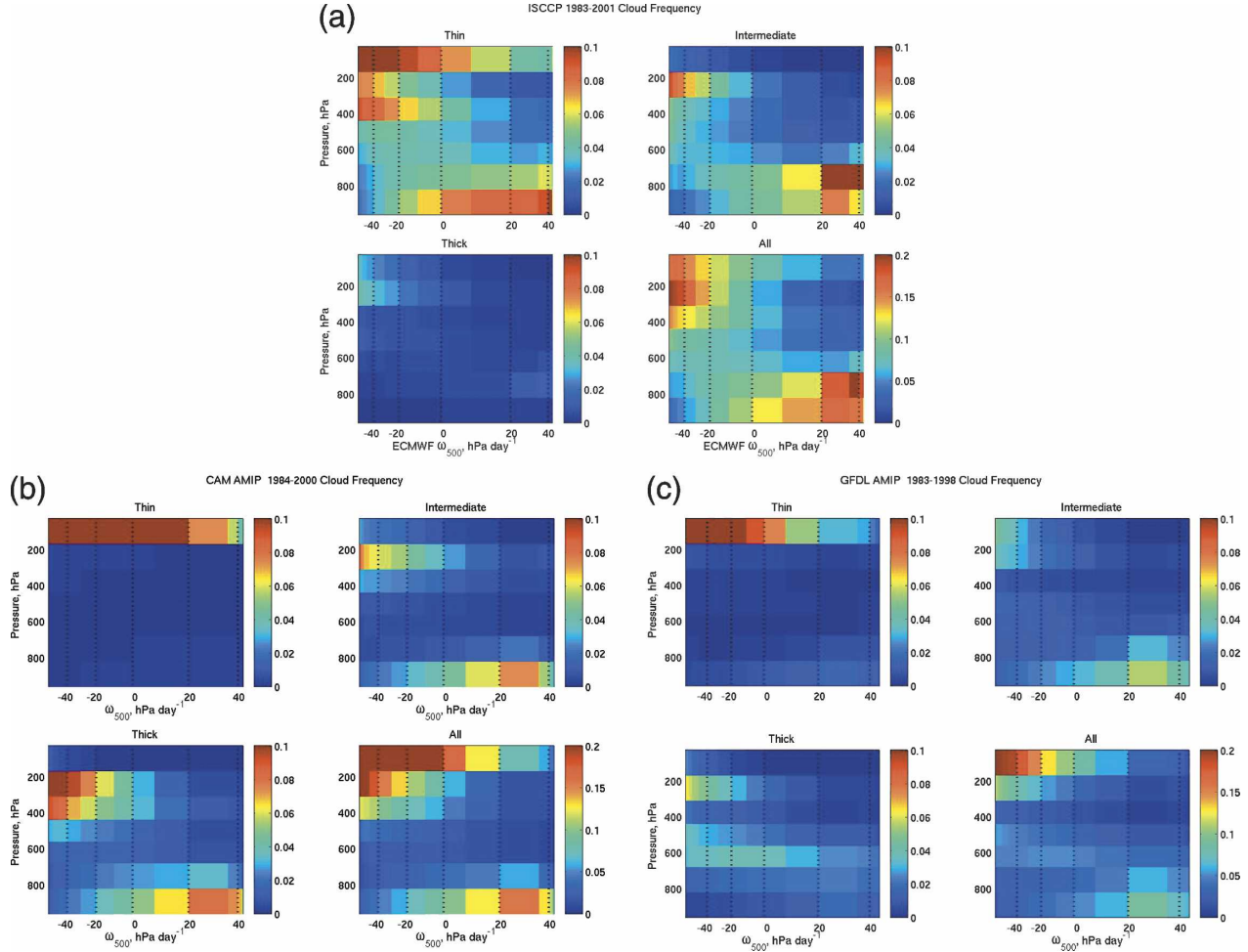
FIG. 11. (a) (top) ISCCP monthly mean cloud frequency sorted using the ω_{500} from ECMWF analysis, and divided into ISCCP cloud thickness categories: thin ($0.02 \le \tau \le 3.6$), intermediate ($3.6 \le \tau \le 23$), thick ($\tau \ge 23$), and (d) all optical depths. (bottom) Monthly mean cloud frequency from the ISCCP simulator for an AMIP simulation of (b) NCAR CAM 3.0 and (c) GFDL AM2.12b climate models over the period 1984–2000, sorted by ω_{500} and using similar thickness categories. (From WYANT.)

of the cloud amount, the cloud thickness, and/or the cloud vertical structure. The simulation of the TOA cloud radiative forcing has generally improved in the current generation of climate models (Lin and Zhang 2004; Zhang et al. 2005). However, models still show substantial disagreement with each other and with ISCCP satellite observations in the cloud fraction, optical thickness, and cloud-top height (Zhang et al. 2005). Figure 11 shows examples of these sorted in dynamical regimes defined using midtropospheric large-scale vertical velocity (WYANT). Moreover, it has been pointed out that models exhibit systematic biases in tropical and midlatitude regions by simulating clouds generally too optically thick, and not abundant enough in the midtroposphere and in large-scale subsidence regimes (Klein and Jakob 1999; Norris and Weaver 2001; Webb et al. 2001; Tselioudis and Jakob 2002; Lin and Zhang 2004; Ringer and Allan 2004; WYANT; Zhang

et al. 2005). In these models, a realistic simulation of the mean cloud radiative forcing at the top of the atmosphere is thus likely to be associated with compensating errors.

The fact that models overpredict cloud optical depth in regimes of strong large-scale ascent occurring in tropical convective regions and midlatitude frontal systems restricts their ability to predict the magnitude of cloud feedbacks. Since cloud albedo is not linearly related to cloud optical depth, small changes in the already excessively large optical depth of the model clouds, even if they are of the right sign and magnitude, or even the right relative magnitude, would produce smaller radiative signatures than similar changes in smaller, more realistic cloud optical depths. This implies that the models lack sensitivity to potential shortwave cloud optical depth feedbacks.

The models' difficulties in simulating the low-level

cloud cover in subsidence regimes also cast doubts on their ability to simulate realistic subtropical cloud feedback processes. Indeed, Bony and Dufresne (2005) show that in the Tropics, most of the GCMs participating in the AR4 of the IPCC underestimate the interannual sensitivity of the cloud radiative forcing to SST changes that occur in regimes of large-scale subsidence and weak precipitation. Given the large contribution of these regimes to the sensitivity of the earth's radiation budget (Norris and Weaver 2001; Bony et al. 2004; Bony and Dufresne 2005; WEBB), this is a concern for the models' estimate of climate sensitivity.

2) DISCRIMINATING BETWEEN CLIMATE CHANGE CLOUD FEEDBACKS BASED ON OBSERVATIONAL TESTS?

The GCMs exhibit a broad range of cloud feedbacks in climate change. They cannot all be right. The hope is thus to find some observational tests or diagnostics, which may be applied to GCMs that may discriminate between the different behaviors of clouds in climate change. This would allow us to assess our confidence in some of the climate change cloud feedbacks, and to observationally constrain the range of global cloud feedbacks.

Williams et al. (2006) show that in doubled-CO_2 experiments performed with slab ocean models, changes in vertical velocity and lower-tropospheric stability can explain most of the spatial cloud response to a doubling of CO_2 over the Tropics and midlatitudes. In each model, this can be quantitatively related to present-day variability, and so evaluated against observational data. Bony and Dufresne (2005) pointed out large intermodel differences in the sensitivity of the SW CRF to SST changes both in climate change and in current interannual variability, in tropical subsidence regimes. They also show that on average (but there is a large variability within the models), the models that predict a large positive anomaly of the SW CRF under climate change tend to better reproduce the interannual CRF sensitivity to SST in subsidence regimes than the models that predict a negative or a weak positive anomaly of the SW CRF under climate change. Further analysis of the reasons for these differences will presumably help to find robust observational tests that may constrain the response of clouds, in particular at low levels, to climate change. To date, however, no test currently applied to GCMs has proved to be discriminating enough to falsify any of the GCMs' cloud feedbacks.

3) MORE GLOBAL INVESTIGATIONS

Tsushima and Manabe (2001) and Tsushima et al. (2005) proposed considering seasonal variations of the current climate to estimate the magnitude of cloud feedbacks. They show that the globally averaged LW and annually normalized SW components of the observed cloud radiative forcing[4] depend little upon the annual variation of global mean surface temperature, and suggest that the LW, SW, and LW + SW (NET) components of the cloud feedback estimated from observations is close to zero. The three atmospheric models considered by Tsushima et al. (2005) reproduce the weak magnitude of the NET seasonal cloud feedback, but fail to reproduce the weak magnitude of the individual LW and SW components. Currently, we have no evidence that the models' cloud feedbacks estimated from seasonal variations resemble those estimated from long-term climate changes associated with greenhouse forcing.

Reproducing the variations of the current climate observed over the last two decades constitutes another critical test for climate models. Current models have been found unable to reproduce the decadal variations of the tropical cloudiness and the earth's radiation budget seen in observations, simulating variations weaker than observed (Wielicki et al. 2002; Allan and Slingo 2002). However, the physical origin and the characterization of these decadal variations remain open issues, and it is too early to assess the implications of this deficiency for the models' estimate of cloud feedbacks.

3. Water vapor–lapse rate feedbacks

a. Basic physical processes

Water vapor absorption is strong across much of the longwave spectrum, generally with a logarithmic dependence on concentration. Additionally, the Clausius–Clapeyron equation describes a quasi-exponential increase in the water vapor–holding capacity of the atmosphere as temperature rises. Combined, these facts predict a strongly positive water vapor feedback providing that the water vapor concentration remains at roughly the same fraction of the saturation specific humidity (i.e., unchanged relative humidity). Indeed, the global warming associated with a carbon dioxide doubling is amplified by nearly a factor of 2 by the water vapor feedback considered in isolation from other feedbacks (Manabe and Wetherald 1967), and possibly by as much as a factor of 3 or more when interactions with other feedbacks are considered (Held and Soden 2000). It has also been suggested that the water vapor feed-

---

[4] Tsushima and Manabe (2001) define the annually normalized SW cloud radiative forcing as the difference between clear-sky and all-sky planetary albedo multiplied by the annually averaged insolation [Eq. (18) of their paper].

back plays an important role in determining the magnitude of natural variability in coupled models (Hall and Manabe 2000). Understanding the physics of that feedback and assessing its simulation in climate models is thus crucial for climate predictions.

Variation with height of the temperature changes induced by an external climate forcing can also constitute a radiative feedback (see appendix A). The tropospheric temperature lapse rate is controlled by radiative, convective, and dynamical processes. At extratropical latitudes, the lapse rate is constrained by baroclinic adjustment (Stone and Carlson 1979). The temperature profile of deep convective atmospheres is nearly moist adiabatic (Xu and Emanuel 1989), and dynamical processes prevent the tropical atmosphere from maintaining substantial horizontal temperature gradients in the free troposphere. As a result, the temperature profile of the free troposphere is close to a moist adiabat throughout low latitudes.

In response to global warming, at low latitudes GCMs predict a larger tropospheric warming at altitudes than near the surface (consistent with the moist adiabatic stratification of the atmosphere), and thus a negative lapse rate feedback. At mid- and high latitudes, on the other hand, they predict a larger warming near the surface than at altitude (i.e., a positive lapse rate feedback). On average over the globe, the tropical lapse rate response dominates over the extratropical response, and the climate change lapse rate feedback is negative in most or all the GCMs (Fig. 1). However, the magnitude of this feedback differs substantially among the models. Intermodel differences in global lapse rate feedback estimates are primarily attributable to differing meridional patterns of surface warming: the larger the ratio of tropical over global warming, the larger the negative lapse rate feedback (Soden and Held 2006).

In the current climate, GCMs simulate a month-to-month variability of tropical temperatures larger at high altitudes than at the surface, in accordance with observations and with theory (Santer et al. 2005). At the decadal time scale, GCMs predict lapse rate changes with surface temperature that are consistent with the temperature dependence of moist adiabats, but there are discrepancies among observational datasets (GCM simulations are consistent with the Remote Sensing Systems satellite dataset, but predict a tropospheric amplification of surface warming that is larger than that suggested by the University of Alabama in Huntsville, Alabama, satellite dataset and by the current best estimates from the radiosonde datasets; Santer et al. 2005). The ability of GCMs to accurately simulate long-term lapse rate variations is thus not firmly established yet. If GCMs were actually found to overestimate the tropical amplification of surface warming on long time scales, this would indicate that the GCMs' lapse rate feedback is too negative in the Tropics, and thus that GCMs' estimates of climate sensitivity are underestimated.

As illustrated in Fig. 12, the free troposphere is particularly critical for the water vapor feedback, because humidity changes higher up have more radiative effect (Shine and Sinha 1991; Spencer and Braswell 1997; Held and Soden 2000; Marsden and Valero 2004; Forster and Collins 2004; Inamdar et al. 2004). In the Tropics, the upper troposphere is also where the temperature change associated with a given surface warming is the largest, owing to the dependence of moist adiabats on temperature. If relative humidity changes little, a warming of the tropical troposphere is thus associated with a negative lapse rate feedback and a positive upper-tropospheric water vapor feedback. As explained by Cess (1975), this explains a large part of the anticorrelation discussed in the introduction between the water vapor and lapse rate feedbacks of climate models (Fig. 1). It explains also why the magnitude of relative humidity changes matters so much for the magnitude of the combined water vapor–lapse rate feedbacks: a change in relative humidity alters the radiative compensation between the water vapor and lapse rate variations, so that an increase (decrease) in relative humidity will enhance (lessen) the water vapor feedback relative to the lapse rate feedback. Note also that changes in tropospheric relative humidity are critical also for cloud feedbacks since they may affect the cloud cover.

As reviewed by Emanuel and Pierrehumbert (1996), Emanuel and Zivkovic-Rothman (1999), Held and Soden (2000), and Stocker et al. (2001), the distribution of humidity within the troposphere is controlled by many factors, including the detrainment of moisture from convective systems (which depends on the penetration height of convective cells, on cloud microphysical processes such as the conversion of cloud water to precipitation or the reevaporation of precipitation, and on turbulent mixing between cloud-saturated and environmental air), and the large-scale atmospheric circulation (Fig. 13). Confidence in GCMs' water vapor feedbacks depends on how much the (parameterized) details of cloud and convective microphysics are critical for simulating the relative humidity distribution and its change under global warming. This issue remains somewhat uncertain. Unidimensional modeling studies have emphasized the sensitivity of the simulated relative humidity distribution to microphysical parameters (Rennó et al. 1994), and it has been suggested that this sensitivity was much weaker at vertical resolutions comparable to those used in GCMs than at high vertical
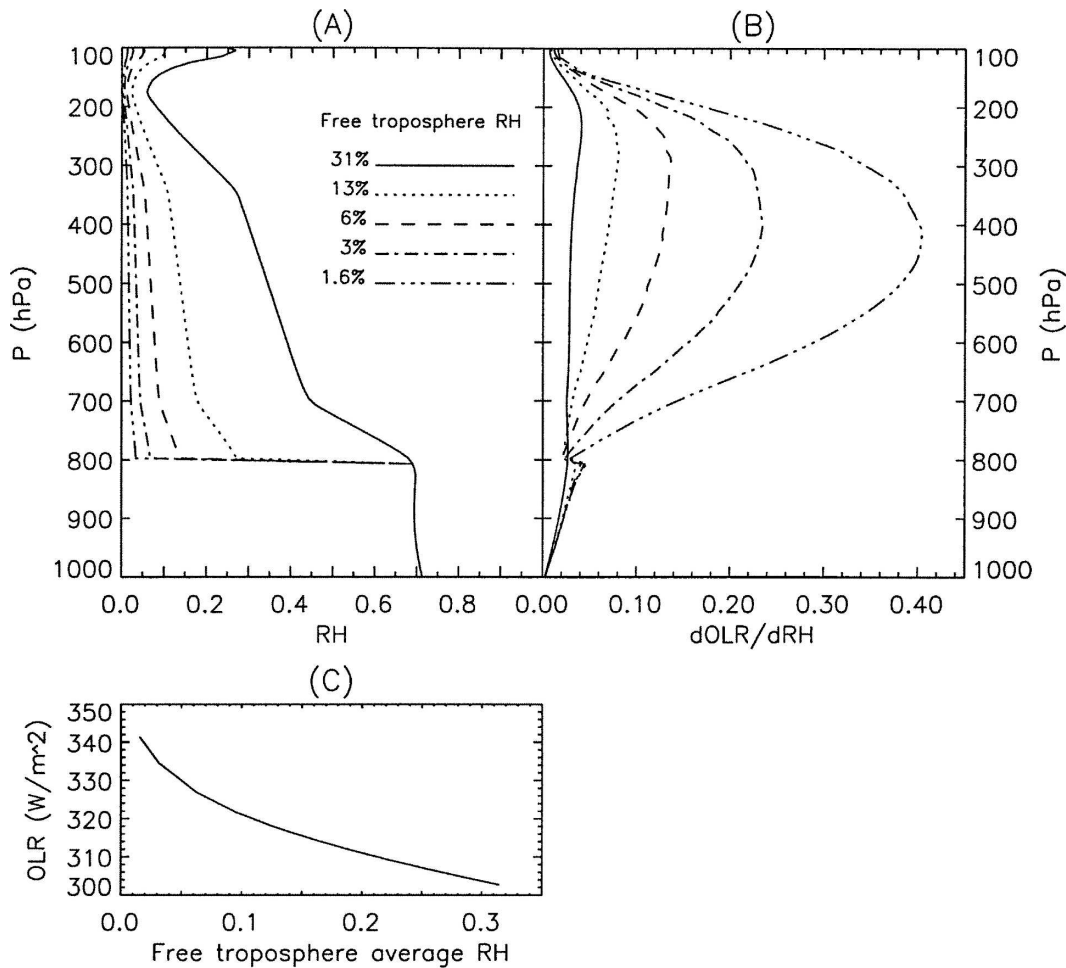
FIG. 12. (a) Progressive humidity profiles computed by reducing the free-tropospheric specific humidity of the Air Force Geophysical Laboratory profile between 800 and 100 hPa by multiplicative factors of 1.0, 0.4, 0.2, 0.1, and 0.05. This results in height-weighted average relative humidities in the free troposphere of 31%, 13%, 6%, 3%, and 1.6%, respectively. (b) Sensitivity of outgoing LW radiation to additive changes of relative humidity of 3% in 10-hPa-thick layers as a function of the humidity profiles shown in (a). (c) The nonlinear dependence of clear-sky outgoing LW radiation over this range of free-tropospheric relative humidity. [From Spencer and Braswell (1997).]

resolutions (Emanuel and Zivkovic-Rothman 1999; Tompkins and Emanuel 2000). In one GCM, however, the water vapor feedback strength has been found to be insensitive to large changes in vertical resolution (Ingram 2002). Several studies have shown that the tropospheric distribution of humidity of the current climate can be well simulated without microphysics, but simply by advection by observed winds while imposing an upper limit of 100% relative humidity to rising parcels (Sherwood 1996; Pierrehumbert and Roca 1998; Dessler and Sherwood 2000). Other studies have also shown that although cirrus might possibly be important as a humidity sink in the upper troposphere, the reevaporation of cirrus clouds in the upper troposphere does not appear to play a major role in moistening (Luo and Rossow 2004; Soden 2004). The critical role that

clear-sky cooling plays in determining moisture detrainment and upper-tropospheric relative humidity distributions has also been emphasized (Iwasa et al. 2004; Folkins et al. 2002). Overall, although different studies suggest that details of the GCMs' representation of cloud microphysical and turbulent processes does not appear crucial to simulate the broadscale upper relative humidity distribution in the current climate, some uncertainty remains as to the role of these processes in the response of the tropospheric relative humidity distribution to climate warming.

Lindzen (1990) argued that the mean detrainment altitude of deep convection might be higher and cooler in a warmer climate, leading to a drying of the upper troposphere and a negative water vapor feedback. Objections to this hypothesis have been raised by several
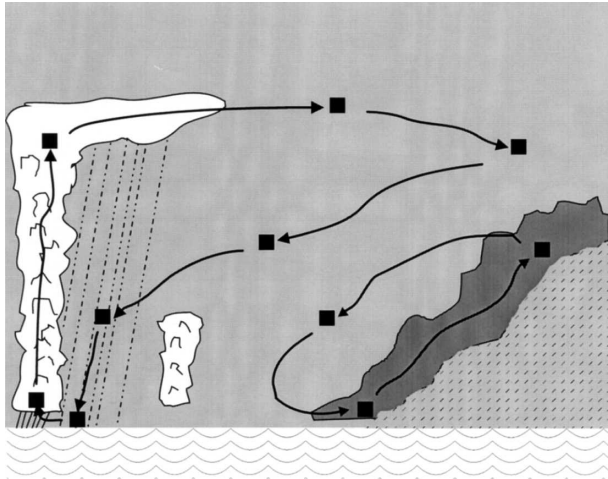
FIG. 13. Illustration of Lagrangian trajectories through the atmosphere, showing the importance of microphysical processes in determining the water content of air. Diagram extends from (left) equator to (right) high latitudes and extends from surface to lower stratosphere. White clouds represent cumuli while the dark cloud represents sloping ascent in baroclinic systems. The total water content of air flowing out of clouds is set by the fraction of condensed water converted to precipitation, and subsequent moistening in the general subsiding branch is governed by detrainment from shallower clouds and by evaporation of precipitation. [From Emanuel and Zivkovic-Rothman (1999).]

studies (e.g., Held and Soden 2000). For instance, Minschwaner and Dessler (2004) show that as the surface warms, warming in the troposphere dominates over higher detrainment, leading to increased upper-tropospheric water vapor and positive water vapor feedback, albeit with a slight decrease of upper-tropospheric relative humidity. It has long been recognized that in GCMs, there can be a reduction in upper-tropospheric relative humidity from changes in detrainment height (Mitchell and Ingram 1992). GCMs do indeed simulate a small, but wide-scale decrease in relative humidity under global warming. While this might potentially play a role in cloud feedback, in GCMs it decreases the water vapor feedback by no more than 5% compared to the case of unchanged relative humidity distribution (Soden and Held 2006).

How may the lower-stratospheric water vapor be affected by a global climate change? The physical mechanisms that control it include chemical, dynamical, and convective processes. It has been suggested that the lower-stratospheric water vapor amount is controlled by the temperature of the tropical tropopause (Moyer et al. 1996; Rosenlof et al. 1997; Joshi and Shine 2003). However, the mechanisms involved are not well understood. This is particularly true of mechanisms through which water vapor is transported from the troposphere to the lower stratosphere: recent observations suggest

that convective and gradual ascent processes, at least, play important roles, but the relative importance of both remains a matter of debate (Keith 2000; Sherwood and Dessler 2000; Webster and Heymsfield 2003; Rosenlof 2003). Given the rudimentary understanding of these processes, it is too early to determine how these processes might be affected by a global climate change. The extent to which stratospheric water vapor changes actually contribute to the water vapor feedback in current climate models will be discussed in section 3f.

b. Observed relative humidity variations

Since the question of whether relative humidity may be altered in a perturbed climate is at the heart of the water vapor–lapse rate feedbacks, several observational studies have investigated how relative humidity changes on interannual to decadal time scales.

When considering large-scale interannual variations of the column-integrated water vapor with sea surface temperature over the last decade, satellite observations suggest a thermodynamic coupling consistent with close to invariant relative humidity (Wentz and Schabel 2000; Trenberth et al. 2005); this behavior is also found in current climate models (Soden and Schroeder 2000; Allan et al. 2003). This tight coupling is unsurprising since most of the columnar water vapor amount lies in the planetary boundary layer, and given the water availability and the near-saturation of the marine boundary layer. At a more regional scale (e.g., in North America or in the western tropical Pacific), however, the relationship between lower-tropospheric humidity and temperature derived from radiosondes has been found to be intermediate between invariant specific humidity and invariant relative humidity, with correlations between interannual anomalies of temperature and relative humidity generally negative and correlations between temperature and specific humidity generally positive (Ross et al. 2002). Satellite measurements of the free-tropospheric relative humidity (FTRH) derived from the High-Resolution Infrared Sounder (HIRS) show that at the regional scale, interannual FTRH variations are closely associated with large-scale circulation changes, particularly in relation with the El Niño–Southern Oscillation (Bates et al. 2001; Blankenship and Wilheit 2001; McCarthy and Toumi 2004) and/or midlatitude planetary waves (Bates and Jackson 2001; Bates et al. 2001).

Since large-scale circulation changes depend on the nature and the time scale of climate variation considered, one may not extrapolate the temperature–water vapor relationships inferred from short-term climate variations to longer climate changes unless differences
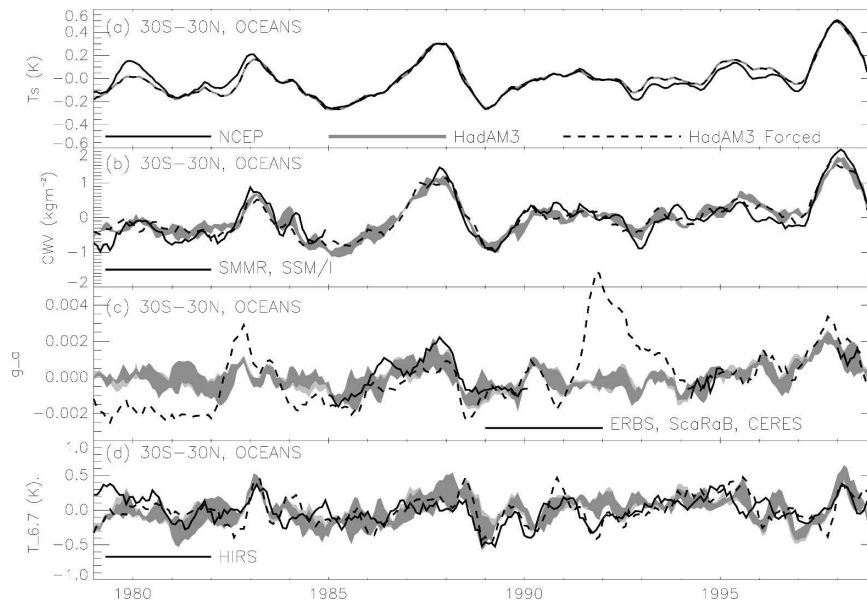
Fig. 14. Interannual variations in (a) surface temperature, (b) column-integrated water vapor, (c) atmospheric normalized greenhouse trapping, and (d) 6.7-μm brightness temperature for the SST-forced model (shaded), model with all known forcings (dashed), and observations (solid). Substantial differences between SST only forced experiments and "full forcing" experiments in (c) indicate that the model normalized greenhouse effect is very sensitive to the input of volcanic aerosols and changes in greenhouse gases. [From Allan et al. (2003).]

in dynamical effects are taken into account (Bony et al. 1995; Lau et al. 1996). To lessen the influence of such effects, relationships may be analyzed by looking at spatial averages over entire circulation systems or by considering dynamical regimes.

When considering averages over the whole Tropics, the FTRH does not vary more than a few percent on interannual to decadal time scales (Bates and Jackson 2001; McCarthy and Toumi 2004). Although ENSO is associated with a change in tropical mean temperature (e.g., Yulaeva and Wallace 1994; Sobel et al. 2002), HIRS data suggest that it is not associated with any substantial change in tropical mean upper-tropospheric relative humidity (McCarthy and Toumi 2004). Nevertheless, the analysis of interannual variations of relative and specific humidity near 215 hPa from Microwave Limb Sounder (MLS) and Halogen Occultation Experiment (HALOE) measurements reveal that an increase in the tropical mean surface temperature of convective regions is associated with an increase of the tropical mean specific humidity but a slight decrease of the tropical mean upper relative humidity (by −4.0 to −8.4% K^{-1}) at 215 hPa (Minschwaner and Dessler 2004).

c. Assessment of models' relative humidity on interannual to decadal time scales

Although not constituting an evaluation of feedbacks, the evaluation of the relative humidity distribu-

tion simulated by models in the current climate provides an integrated and indirect assessment of their ability to represent key physical processes that control water vapor. Minschwaner et al. (2006) show that the AR4 coupled ocean–atmosphere models simulate an increase of specific humidity and a slight decrease of relative humidity at 250 hPa in response to increased surface temperatures in tropical convective regions, in qualitative agreement with observations. Although the models' decreases in relative humidity are not as large as inferred from observation (thus, the GCMs' feedbacks are stronger), the ensemble mean is consistent with observation within the range of combined uncertainties.

The space–time variations of the clear-sky outgoing longwave radiation (OLR) at the TOA are radiative signatures of the humidity and temperature variations and are well measured from space. As illustrated by Fig. 14, several model–data comparisons indicate that models can reproduce the interannual and decadal variations in clear-sky OLR measured by satellite instruments (Soden 2000; Allan and Slingo 2002); although differences in the observed and simulated aerosol or greenhouse gas concentrations and the sampling of clear skies can affect these comparisons (Allan et al. 2003).

There has been substantial effort during the last few years to assess variables more closely related to the
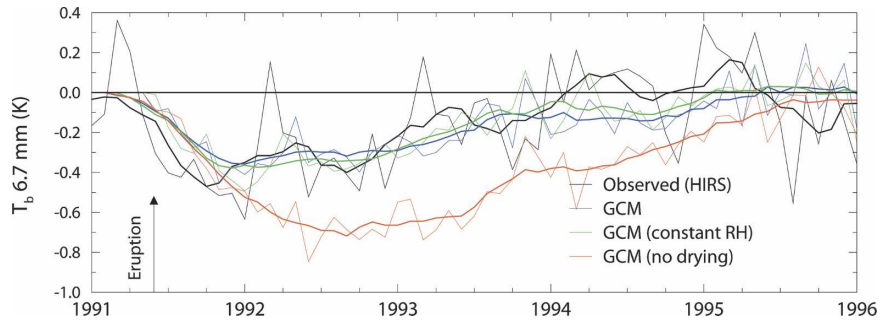
FIG. 15. Comparison of the observed (black) and GCM-simulated (blue) changes in global-mean (90°S–90°N) 6.7-μm brightness temperature (T_b6.7). The observed anomalies are computed with respect to a 1979–90 base climatology and expressed relative to their preemption (January–May 1991) value. The GCM-simulated anomalies are computed as the ensemble-mean difference (Pinatubo − control) from three pairs of GCM simulations. The green curve depicts the GCM-simulated T_b6.7 computed under the assumption of a constant relative humidity change. The red curve depicts the GCM-simulated T_b6.7 computed under the assumption of a constant, seasonally varying water vapor mixing ratio (i.e., no drying of the upper troposphere). The thick lines depict the 7-month running mean of each time series. [From Soden et al. (2002).]

tropospheric relative humidity. In particular, the 6.7-μm radiances observed from satellites have been compared with those simulated from models by following a model-to-satellite approach (such an approach reduces the errors in converting the radiance to model-level relative humidity (Iacono et al. 2003; Allan et al. 2003). Allan et al. (2003; Fig. 14 of this paper) found that one model simulated long-term climatology and its small interannual and decadal variations in relative humidity in broad agreement with the observational record from HIRS. Iacono et al. (2003), also analyzing HIRS radiances, noted substantial bias in the simulation of upper-tropospheric humidity by another model. Brogniez et al. (2005) show that current atmospheric models reproduce fairly well the seasonal and interannual variations of upper relative humidity when compared to Meteosat water vapor channel data over the Atlantic region. However, they show that most models simulate too moist an upper troposphere in subsidence regions.

Given the near-logarithmic dependence of longwave radiation on water vapor amount, the impact of mean biases in the simulation of upper relative humidity on the models water vapor feedback is likely to be small *if* relative humidity is nearly constant under climate change (Held and Soden 2000). Nevertheless, the radiative impact of small changes in relative humidity is expected to be slightly underestimated (overestimated) in regions of moist (dry) bias.

d. Pinatubo and water vapor feedback

Recently, there have been attempts to assess the global water vapor feedback by examining global cli-

mate variations associated with the Pinatubo volcanic eruption (Soden et al. 2002; Forster and Collins 2004), despite the difficulty in separating the forced climate response from natural climate variability such as ENSO (Forster and Collins 2004). Soden et al. (2002) found the global response of the HIRS 6.7-μm radiance to be consistent with unchanged upper-tropospheric relative humidities (Fig. 15). Using radiation calculations based on water vapor observations, Forster and Collins (2004) found that mid- to upper-tropospheric changes dominated the feedback response, and deduced an estimate of the water vapor feedback parameter (Fig. 16) ranging from 0.9 to 2.5 $Wm^{-2} K^{-1}$ (using the sign convention of Colman 2003a, appendix A, and Fig. 1; i.e., positive feedbacks have a positive sign).

Soden et al. (2002) and Forster and Collins (2004) proposed to take advantage of the global climate perturbation associated with Pinatubo to test the water vapor feedback of climate models. Soden et al. (2002) found consistency between model and observed reductions in lower- and upper-tropospheric moisture in response to the global-scale cooling (Fig. 15). Using an ensemble of coupled climate model integrations, Forster and Collins (2004) found consistency between model water vapor feedback and that deduced from Pinatubo observations, although there is considerable uncertainty due to variability unrelated to the volcanic forcing. Nevertheless, they showed that the latitude–height pattern of the observed water vapor response following the eruption differed from that found in any integration of the model in the ensemble.

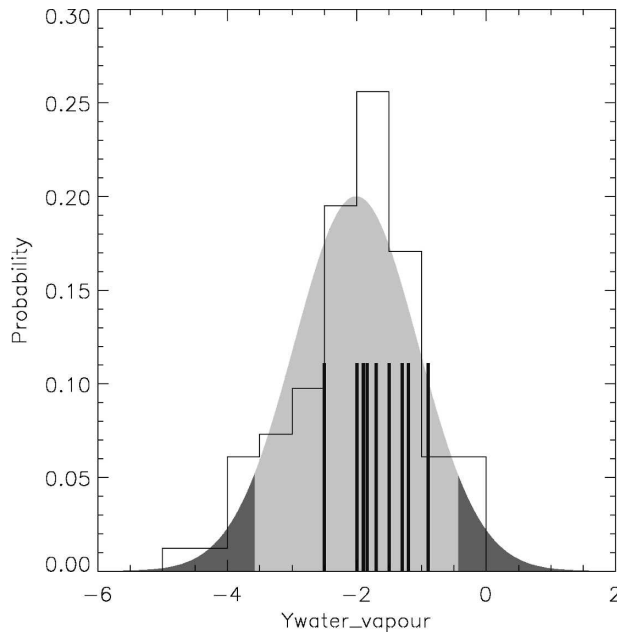Volcanic eruptions appear to constitute useful obser-

FIG. 16. Estimates of water vapor feedback parameter (in W m^{-2} K^{-1}) from the observations and from the HadCM3 climate model (note that the sign convention used in this figure for the definition of feedback parameters is opposite to that used in appendix A). The histogram is computed from 82 model estimates with a bin size of 0.5 and is shown in terms of probabilities. The shaded curve is a fitted normal distribution of model estimates with the 5% and 95% represented by darker shading. Observed estimates of the water vapor feedback parameter are indicated by the vertical lines, and lie in the range 0.9–2.5 W m^{-2} K^{-1} (using the sign convention of appendix A, i.e., positive feedbacks have positive sign). [From Forster and Collins (2004).]

vational tests of the climate response to a specified radiative forcing. However, caution is required before drawing extrapolations to global climate changes associated with increasing greenhouse gases. Indeed, the radiative forcing associated with an eruption such as Pinatubo is less globally uniform than that associated with an increase of greenhouse gases concentration. Therefore the climate anomaly associated with Pinatubo volcanic forcing has a different geographical structure and may involve different feedbacks than the climate anomaly associated with greenhouse forcing. Moreover, volcanic aerosols primarily reduce the incoming SW radiation at the surface, while greenhouse gases increase the atmospheric trapping of LW radiation: both forcings have thus different vertical distributions, the SW perturbation being felt primarily at the surface and the LW perturbation within the troposphere. The SW and LW forcings of similar sign and magnitude may ultimately lead to surface temperature changes of same sign. However, several studies have shown that the response of the hydrological cycle de-

pends on the nature of the perturbation imposed (Hansen et al. 1997; Allen and Ingram 2002; Joshi et al. 2003; Yang et al. 2003). Although differences are expected to be the largest at short time scales, the equilibrium response might differ too: Hansen et al. (1997) and Joshi et al. (2003) found a climate sensitivity 20% weaker in the case of a SW perturbation than in the case of an equivalent LW perturbation. In addition, Hallegatte et al. (2006) give an estimate of 4–7 yr for the buildup duration of the water vapor feedback. It means that the amplification due to the water vapor feedback in response to a perturbation shorter than one decade is weaker than the amplification in response to a permanent perturbation (even in relative terms). This long duration can be explained by the fact that the feedback is mediated by successive short but nonzero characteristic time processes (ocean warming, latent and radiative flux changes, etc.). Such a long time scale suggests that even the water vapor feedback may not be fully active over the years immediately following the eruption.

Therefore, although the climate response to volcanic eruptions provides useful tests of the ability of climate models to reproduce some specific aspects of the climate response to a given forcing, or some particular physical processes involved in climate feedbacks, it certainly cannot be considered as an analog of the climate response to long-term increases in greenhouse gases.

e. Could the weak relative humidity response be an artifact of climate models?

Climate models produce a range of interannual responses of the vertical profiles of temperature and moisture when regressed onto surface temperatures (Hu et al. 2000; Allan et al. 2002). This likely relates to differences in physical parameterizations, and probably explains in part the spread in the water vapor and lapse rate feedbacks shown in Fig. 1. However, models containing a wide range of parameterizations predict a small variation in the global-mean relative humidity under climate change, inducing a strongly positive water vapor feedback (Held and Soden 2000; Colman 2003b, 2004). Therefore, one may wonder whether this is an artifact of all climate models, or whether this is a robust feature of climate change.

A possible artifact of climate models' simulation of water vapor might be associated with the lack of vertical resolution in the free troposphere, as Tompkins and Emanuel (2000) found that a vertical resolution better than 25 hPa was required to get numerical convergence in the simulation of the tropical water vapor profile. But Ingram (2002) found no significant change in a

model's water vapor feedback by replacing the number of vertical levels between 11 and 100, nor by changing the convection scheme of the model. An analysis of the correlation between interannual variations of large-scale average temperature and water vapor suggested that the correlation was stronger and less height dependent in GCMs than in radiosonde observations (Sun et al. 2001). But that result was questioned by Bauer et al. (2002), who found that allowing for sampling biases in the observations reduced the discrepancy between observed and simulated correlations from about 0.5 to about 0.2. Considering the uncertainty in radiosonde upper-tropospheric humidity measurements, they further questioned whether the remaining differences mattered. They also showed that the models' correlation between temperature and water vapor was insensitive to the choice of the convection scheme. In cloud resolving (Tompkins and Craig 1999) and mesoscale (Larson and Hartmann 2003) model experiments, a relative humidity response close to unchanged is found also at almost all levels of the troposphere under climate warming.

Therefore, although models do not explicitly fix relative humidity at a constant value, their prediction of a nearly unchanged mean relative humidity under climate warming is a robust feature of climate change predictions. Based on recent studies, no substantive evidence suggests that the weak relative humidity response of climate models, and thus the large magnitude of the water vapor–lapse rate feedback under climate change, are an artifact of climate models. However, as the water vapor feedback represents the strongest positive feedback of the climate system, uncertainties about *how small* relative humidity changes should be, or *how accurate* the magnitude of the correlation between humidity and temperature should be, can matter for the spread in water vapor–lapse rate feedback and for the magnitude of climate sensitivity (Fig. 1). For instance, examining relationships at individual stations rather than in zonal averages, Ross et al. (2002) showed that in some atmospheric GCMs participating in the Second Atmospheric Models Intercomparison Project (AMIP-II), the correlation between temperature and lower-tropospheric humidity was slightly stronger than observed at high latitudes and over the eastern United States. The quantitative impact that such inaccuracies might have on model estimates of climate sensitivity is currently unknown.

In consequence, further and more quantitative investigations are required to assess factors that may produce relative humidity variations. Among these processes, one may consider in particular the sensitivity of convective cloud microphysics to temperature, a factor poorly represented in current convection schemes (Emanuel and Zivkovic-Rothman 1999), and the response of the large-scale tropical circulation to global warming. Indeed, cloud-resolving simulations of Peters and Bretherton (2005) suggest that the region of deep convection slightly narrows in a warmer climate, producing a climate sensitivity somewhat less than would be predicted for a cloud-free, moist-adiabatically stratified, constant relative humidity atmosphere.

f. Lower-stratospheric water vapor

To what extent do lower stratospheric water vapor changes contribute to climate feedbacks? Actually, they do not sit easily within the conceptual framework that distinguishes radiative forcing and climate feedback: as explained by Forster and Shine (1999), stratospheric water vapor changes resulting from methane oxidation will be considered as part of the forcing, whereas those associated with a change in the tropopause temperature will be considered as part of the climate response and feedbacks. Irrespective of whether it is considered part of the radiative forcing or of the climate response, it can be shown that an increase in stratospheric water vapor leads to stratospheric cooling and to surface and tropospheric warming (Rind and Lonergan 1995). However, the resemblance with the impact of tropospheric water vapor is limited for several reasons. First, for the same fractional change in water vapor, lower-stratospheric water vapor changes affect the earth's radiation budget at the top of the atmosphere much less than mid- to upper-tropospheric water vapor changes (Allan et al. 1999). Second, there is no reason to expect the stratospheric relative humidity to be roughly unchanged in conditions so far from saturation, so the size of the stratospheric water vapor changes are not expected to be even roughly proportional to the local or near-surface warming, as confirmed by the simulations of Stuber et al. (2001). These show that the change in the stratospheric water vapor induced by ozone perturbations in the lower stratosphere surpasses by an order of magnitude the water vapor change induced by ozone perturbations in the upper troposphere or that induced by an equivalent CO_2 perturbation.

As a result, the contribution of lower-stratospheric water vapor changes to climate sensitivity is highly dependent on the nature of the climate perturbation. Experiments in which equivalent (1 W m^{-2}) lower stratospheric ozone and homogeneous CO_2 forcing were applied to a GCM found that suppressing the radiative impacts of stratospheric water vapor changes reduced global surface warming by 40% in the case of the ozone
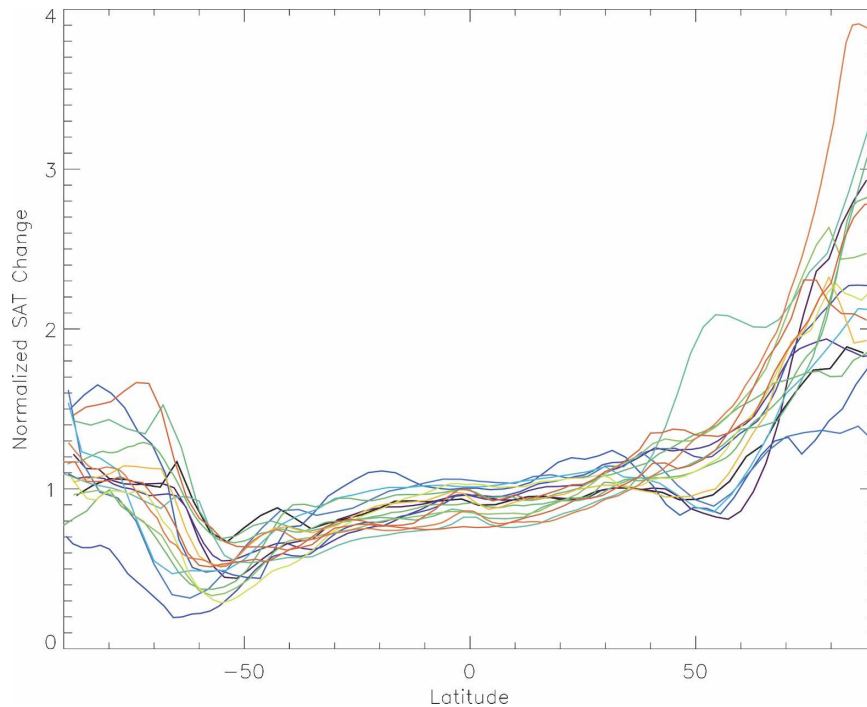
FIG. 17. The normalized zonally averaged surface air temperature change from 17 models participating in the AR4 of the IPCC. The temperature change is computed as the 2080–99 average from the so-called SRES AlB scenario minus the 1980–99 average from climate of the twentieth-century simulations. The zonally averaged change is normalized by the global average surface air temperature change.

perturbation, but only around 1% for the CO_2 perturbation (Stuber et al. 2001). In conclusion, water vapor changes in the lower stratosphere may not greatly affect the magnitude of the global water vapor feedback in the case of a CO_2 doubling. However, assessing the mechanisms that control the change in stratospheric water vapor is crucial for understanding and predicting the evolution of the chemical composition of the lower stratosphere.

4. Cryosphere feedbacks

Polar regions are characterized by complex and still insufficiently understood feedbacks in the climate system. Many of these feedbacks are introduced by the cryosphere and, in particular, by sea ice with all the complexities of its thermodynamics and dynamics. A robust feature of the response of climate models to increases in atmospheric concentrations of greenhouse gases is the poleward retreat of snow and ice, and the polar amplification of increases in lower-tropospheric temperature. This is particularly true in the Northern Hemisphere. High southern latitudes can exhibit relatively small changes in surface air temperature, due to

high ocean heat uptake in these regions (note, however, that this is a feature of transient climate change, since in equilibrium climate change experiments the Southern Hemisphere exhibits just about as much poleward amplification as the Northern Hemisphere).

Polar amplification is usually attributed to positive feedbacks in the climate system, the cryosphere being of prime importance. The cryosphere feedbacks are strongly coupled to processes in the atmosphere and ocean (e.g., polar cloud and radiation processes and ocean heat transport). To what extent polar amplification is due to real physical processes rather than to model imperfections remains an open question. Notably, it is in high latitudes, that climate models demonstrate the largest intermodel scatter in quantification of the greenhouse gas–induced climate change. For example, in northern high latitudes, the warming simulated at the end of the twenty-first century by current models ranges from 1.3 to almost 4 times the global mean warming (Fig. 17).

Radiative feedbacks associated with the cryosphere, which we focus on here, are widely accepted to be major contributors to polar amplification. However, they are apparently not the only ones. For example, feed-

backs associated with atmospheric dynamics and heat transport, which are not directly dependent on snow or ice, can contribute to polar amplification (e.g., Alexeev 2003; Alexeev et al. 2005). In general, the present-day physical understanding of processes contributing to (or moderating) polar amplification and the interdependence among those processes has not been clearly quantified.

a. Snow feedbacks

The main simulated feedback associated with snow is an increase in absorbed solar radiation resulting from a retreat of highly reflective snow in a warmer climate. This process, known as snow albedo feedback, enhances simulated warming and contributes to poleward amplification of climate change. In the Southern Hemisphere, the effect of snow retreat on polar amplification is negligible compared to that of the sea ice retreat, as comparatively little snow cover exists in the midlatitudes of the Southern Hemisphere, and the snow on the Antarctic ice sheet remains frozen nearly all year-round. In the Northern Hemisphere by contrast, the current generation of GCMs participating in the AR4 of the IPCC indicate that approximately half the simulated annual-mean increase in solar radiation resulting from the shrunken cryosphere is due to snow retreat, and half to sea ice retreat (Winton 2006).

Previous work showed that snow albedo feedback to anthropogenic climate change was generally positive in the then-current generation of GCMs, but that estimates of its strength vary widely (Cess et al. 1991; Randall et al. 1994). Moreover, interactions between snow and other factors such as clouds sometimes generated weak negative feedbacks associated with snow changes.

Recent studies have brought new evidence that Northern Hemisphere snow albedo feedback is positive in the real world. Examining output from an atmospheric GCM forced by observed SSTs, Yang et al. (2001) showed that the large surface air temperature anomalies over North America associated with the ENSO phenomenon agree well with the observed temperature anomalies when snow albedo feedback is present, but are reduced by more than half over most of the continent when snow albedo feedback is suppressed. Therefore the simulation requires positive snow albedo feedback to simulate realistic ENSO climate impacts. Analyzing the two-decade-long satellite-based ISCCP dataset, Qu and Hall (2005) demonstrated that snow albedo anomalies account for more than half the variability in planetary albedo in snow-covered regions throughout nearly the entire year, showing their importance despite cloud masking. This corroborates work by Groisman et al. (1994), who showed that snow variability influences planetary albedo variability even in cloudy regions. This suggests a retreat of Northern Hemisphere snow cover would result in a substantial reduction in the planet's top-of-the atmosphere albedo, a necessary precondition to positive snow albedo feedback.

In spite of these advances, Northern Hemisphere snow albedo feedback remains subject to considerable uncertainty and is therefore a likely source of divergence and errors in models. Recent attempts to quantify snow albedo feedback in models for comparison with observations involve breaking it down into its two constituent components, one relating the surface albedo anomalies in snow regions to planetary albedo anomalies, and another relating the magnitude of snow albedo anomalies to the surface air temperature anomalies associated with them. The product of these two components is a measure of snow albedo feedback. Differences in both these two quantities between models and observations will result in divergence in simulations of snow albedo feedback.

1) EFFECT OF SURFACE ALBEDO ON PLANETARY ALBEDO IN SNOW REGIONS

Qu and Hall (2006) showed that in the observed satellite record, surface albedo anomalies in either North American or Eurasian snowpacks do affect the TOA albedo. But because the atmosphere also interacts with solar photons, the TOA signature of the surface anomalies is attenuated, with the planetary albedo anomaly typically being about half as large as that of the surface (Fig. 18). They also demonstrated that the current generation of GCMs participating in the AR4 of the IPCC agree with this result to within 10% for the current climate, in spite of substantial differences between models and between models and observations in cloud fields over snow-covered regions. In addition, they showed that the magnitude of the attenuation effect changes little in simulations of future climate, in spite of changes in cloud fields in snow-covered regions. The reason for the agreement between models and observations in the current climate and the near constancy of this effect as climate changes is that the clear-sky atmosphere is responsible for more than half the attenuation effect, so that errors or changes in cloud fields (typically as large as 20%) result in fluctuations smaller than 10% in the attenuation effect. This implies that the relationship between snow albedo and planetary albedo is a reasonably well-known quantity, is unlikely to change much in the future, and is therefore not a significant source of error in simulations of snow albedo feedback.
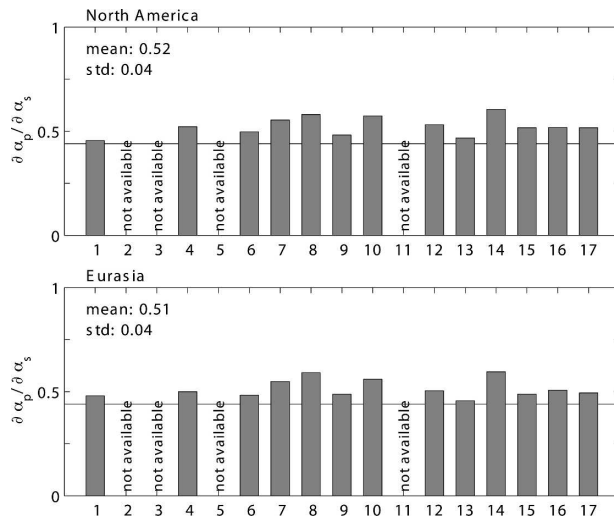
FIG. 18. The dependence of planetary albedo on surface albedo in (top) North American and (bottom) Eurasian landmasses poleward of 30°N during Northern Hemisphere spring, when snow albedo feedback is strongest. Shown with solid horizontal lines are values calculated for the satellite-based ISCCP dataset, covering the 1984–2000 period. Shown with gray bars are values based on the twentieth-century portion of the transient climate change experiments of the AR4 assessment. This shows how large a typical planetary albedo anomaly is for a 1% surface albedo anomaly. In observations, and in all climate simulations, planetary albedo anomalies are consistently about half as large as their associated surface albedo anomalies. Values are available only for 13 of the 17 experiments because 4 of them do not provide all variables required for the calculation. [From Qu and Hall (2006).]

2) RELATIONSHIP BETWEEN SURFACE ALBEDO AND TEMPERATURE IN SNOW REGIONS

The relationship between surface albedo and temperature in snow regions, arising from the way GCMs parameterize snow albedo, is the main source of divergence and error in models. As seen in Fig. 19, there is a spread of more than a factor of 3 in this quantity over both the North American and Eurasian landmasses. Most GCMs parameterize snow albedo as a monotonic function of snow depth and snow age. Though these quantities are no doubt important determinants of snow albedo, snow albedo parameterizations in many state-of-the-art GCMs still do not contain many other processes known to affect snow albedo. Notable among these are snow–vegetation canopy interactions (principally the effect on surface albedo of snow falling off trees within a day or two of snowfall), and the effect of subgrid-scale snow-free surfaces, which can act as seeding areas for snowmelt as temperatures rise. As snow ages, its albedo also decreases even if no melting occurs because the snow crystals change shape and bond together, producing a darker surface (Gray and Landine 1987; Nolin and Stroeve 1997). The effect of impurities
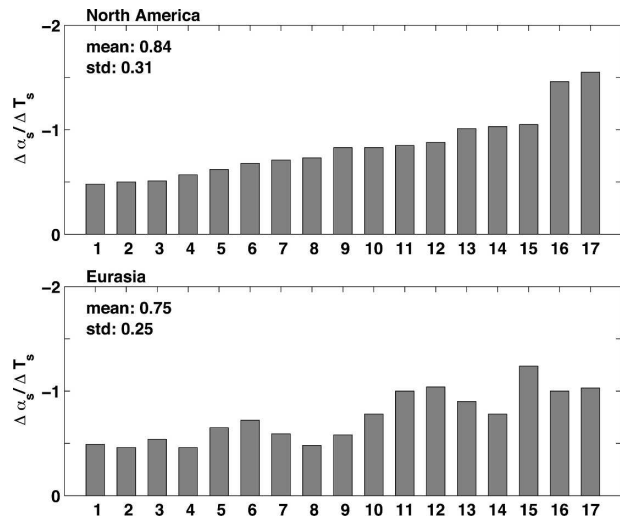
FIG. 19. The externally forced change in springtime surface albedo (%) in snow-covered regions in the transient climate change experiments of the AR4 of the IPCC, divided by the change in springtime surface air temperature (°C) in these experiments, a measure of the surface component of simulated springtime snow albedo feedback: (top) The North American landmass and (bottom) the Eurasian landmass. There are 17 transient climate change experiments, each consisting of a GCM forced by observed changes and future projections of greenhouse gases and other forcing agents. The change in area-mean surface albedo (surface air temperature) is defined as the difference between area-mean surface albedo (surface air temperature) averaged over the twenty-second century of the simulations and the area-mean surface albedo (surface air temperature) averaged over the twentieth century of the simulations. Values of surface albedo were weighted by climatological incoming solar radiation at the surface in the climate of the twentieth century prior to area averaging. (top) Ordered by increasing feedback strength, and this order was preserved in (bottom). The fact that the feedback strength also generally increases in the (bottom) suggests a consistency in the strength of the feedback between the landmasses within any single model. [From Qu and Hall (2006).]

on snow albedo may also be significant. For example, Hansen and Nazarenko (2004) estimated the effect of soot in snow on snow albedo has resulted in a radiative forcing for the Northern Hemisphere on the order of a third of a watt per meter squared. A systematic evaluation of the effects of these additional processes on snow albedo and snow albedo feedback has not been done, so it is not known to what extent their absence is responsible for divergence in simulations of future climate.

A complementary approach to evaluating how much complexity is required to simulate snow albedo processes realistically is direct comparison of surface albedo–temperature relationships in snow areas in simulations to those seen in the real world. Hall (2004) showed that in a coupled ocean–atmosphere model

anomalies of Northern Hemisphere snow cover are approximately the same for a given magnitude of overlying surface air temperature anomaly, whatever the source of the temperature anomaly. This holds even for time scales as short as the seasonal time scale, raising the possibility that the behavior of snow albedo feedback in the context of observed present-day climate variability might prove a meaningful analog to its behavior in anthropogenic climate change. This is confirmed by Hall and Qu (2006) who find that for the GCMs participating in the AR4 of the IPCC, the snow albedo feedback simulated in the context of the present-day seasonal cycle is an excellent predictor of snow albedo feedback in the transient climate change context. This suggests that if climate simulations were constrained to reproduce the observed behavior of snow albedo feedback in the present-day seasonal cycle, it would significantly reduce the divergence in these simulations' snow albedo feedback to the anthropogenic climate change seen in Fig. 19.

b. Sea ice feedbacks

There are a number of important feedbacks associated with sea ice that influence projected climate sensitivity. The net effect is such that changes in sea ice contribute to a projected amplification of climate warming in the Arctic region (e.g., Holland and Bitz 2003; Rind et al. 1995). They also contribute to the global mean warming. For example, Rind et al. (1995) showed that 20%–40% of the simulated global surface air temperature increase at $2 \times CO_2$ conditions was associated with changes in the ice cover. However, the sea ice system is complex and the quantitative influence of the myriad feedbacks associated with sea ice is unclear. The possibility of threshold behavior also contributes to the uncertainty of how the ice cover may evolve in future climate scenarios. These uncertainties contribute to a spread in model projections of Arctic surface air temperature change, which is larger than anywhere else on the globe (Fig. 17).

During the last few years, considerable progress has been made in improving sea ice model physics in coupled ocean–atmosphere general circulation models. For example, most of the models participating in the IPCC AR4 include a representation of sea ice dynamics. Several of these models also include a parameterization of the subgrid-scale distribution of ice thickness and multilayer thermodynamics. In addition to model improvements, there has also been progress in understanding sea ice–related feedbacks. Here we report on the progress at understanding and simulating radiative feedbacks associated with the sea ice. Much work has also examined nonradiative sea ice feedbacks (e.g.,

L'Heveder and Houssais 2001; Holland et al. 2001; Bitz and Roe 2004) but this is beyond the scope of this paper.

1) RADIATIVE FEEDBACKS ASSOCIATED WITH SEA ICE

Arguably the most important sea ice feedback is the influence of the ice area and surface state on the surface albedo. As sea ice melts under a climate-warming scenario, the highly reflective surface is lost, allowing increased solar absorption. This enhances the initial warming perturbation, resulting in a positive feedback. The influence of the albedo feedback on climate simulations has been considered in a number of studies (e.g., Spelman and Manabe 1984; Dickinson et al. 1987; Washington and Meehl 1986; Ingram et al. 1989; Hall 2004). Hall (2004) found that the albedo feedback was responsible for about half the high-latitude response to a doubling of CO_2. However, an analysis of long control simulations showed that it accounted for little internal variability.

Sea ice also affects the surface energy budget by insulating the overlying atmosphere from the relatively warm ocean. As such, the extent and thickness of sea ice modifies the turbulent heat fluxes at the surface. This results in a redistribution of heat in the system. As discussed by Hall (2004) and confirming earlier results by Manabe and Stouffer (1980) and Robock (1983), this feedback is responsible for the seasonal distribution of Arctic warming that is projected by climate models. Although this is not strictly a radiative feedback, it is important for the climate response to the sea ice albedo feedback. While most of the extra absorption of sunlight occurs in summer, much of the additional heat during this time is used for ice melt or ocean surface warming. The atmosphere then responds during fall and winter to the reduced ice thickness, increased open-water areas, and increased sensible heat fluxes, resulting in a maximum warming during this time.

2) INFLUENCE OF MODEL PARAMETERIZATIONS ON SIMULATED SEA ICE RADIATIVE FEEDBACKS

Significant progress has been made over the last few years in our understanding of sea ice related feedbacks. Sea ice model components of coupled atmosphere–ocean general circulation models (AOGCMs) have also improved considerably. For example, most of the models participating in the IPCC AR4 include a representation of sea ice dynamics, which allows for more realism in important ice–ocean exchange processes. However, Flato (2004) in an analysis of the Second CMIP
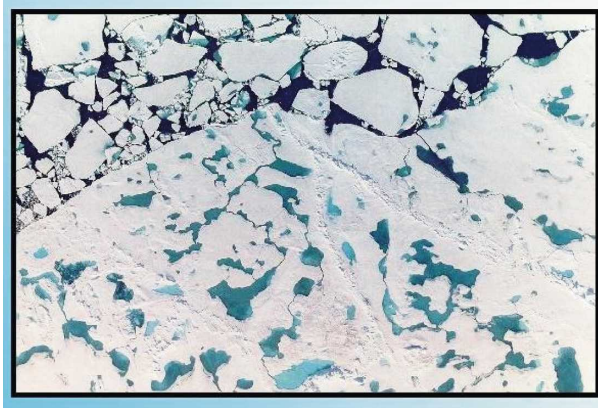
FIG. 20. A photograph of the sea ice surface state taken during the melt season of the Surface Heat Budget of the Arctic Ocean (SHEBA) field program. [From Perovich et al. (1999).]

(CMIP2) simulations found little indication that changes in sea ice model physics were related to an improved simulation or a consistent climate response to increasing CO_2 levels. This suggests that the attributes of the sea ice model physics are secondary to feedbacks and biases involving the atmosphere and ocean. The ice model simulations were quite poor in the CMIP2 simulations. As atmosphere and ocean models improve and represent the climate system with better accuracy, the representation of sea ice model physics may become increasingly important.

A number of coupled GCMs have used recently observed sea ice albedo datasets (e.g., Perovich et al. 2002) to improve their sea ice albedo parameterizations. As shown in Fig. 20, the sea ice surface state can be very complex, with regions of snow-covered ice, surface meltwater ponds, meltwater drainage channels, ridged ice cover and leads, all existing in a relatively small (subGCM grid cell) area. These features modify the surface albedo and are represented to varying degrees in albedo parameterizations used in climate models. The influence that various albedo parameterizations have on simulated feedbacks has been addressed by Curry et al. (2001) using single-column modeling studies. They found that although simulations with different albedo parameterizations may result in similar mean climate conditions, the climate response and strength of feedback mechanisms can be considerably different. Simulations that used a more complex and complete albedo parameterization obtained a considerably stronger albedo feedback. More work is needed to determine if these results extend to coupled global model simulations.

The spatial variations in the surface sea ice state exhibited in Fig. 20 are indicative of high spatial variability that is also present in ice thickness, with thicknesses ranging from open water to thick pressure ridges over regions that are subgrid scale for climate models. Several current models include a representation of the subgrid-scale ice thickness distribution (ITD) developed initially by Thorndike et al. (1975) and adapted for climate models by Bitz et al. (2001). It has long been recognized that the ITD modifies ice growth rates and ice–atmosphere exchange (e.g., Maykut 1982). As such, this parameterization can modify simulated sea ice feedbacks. In coupled general circulation modeling studies, Holland et al. (2005) found that, by resolving thin ice cover, the ITD enhanced the positive surface albedo feedback. This has the potential to modify climate variability and sensitivity, but the net influence depends on the interplay between these and other feedback mechanisms. It appears that this interplay may vary for different forcing scenarios.

5. Summary and conclusions

Climate sensitivity estimates critically depend on the magnitude of climate feedbacks, and global feedback estimates still differ among GCMs despite steady progress in climate modeling. This constitutes a major source of uncertainty for climate change projections. This paper shows that the numerous observational, numerical, and theoretical studies carried out over the last few years have led to some progress in our understanding of the physical mechanisms behind the global estimates of climate feedbacks, that offer promising avenues for the evaluation of the realism of the climate change feedbacks produced by GCMs.

a. Cloud feedbacks

Global cloud feedbacks are still associated with a large range of estimates among GCMs, larger than that of other feedbacks (Fig. 1). Evaluating the feedbacks produced by the different models is thus crucial to narrow the range of climate sensitivity estimates. Real advances in the evaluation of cloud feedbacks have long been hindered by our lack of understanding of the physical processes implicated in these feedbacks. In that regard, progress has been made over the last few years.

• To better understand what controls the climate change cloud feedbacks, simple conceptual frameworks have been used to analyze the complexity of the climate system and to decompose the global cloud feedback into components related to specific physical processes (section 2a). This makes the study of cloud feedbacks more tractable and helps to suggest specific and targeted diagnostics for data analysis and model–data comparison.

- New methodologies of model–data comparison (e.g., model-to-satellite approaches using the ISCCP simulator) and many new diagnostics devoted to the analysis of specified components of cloud feedback mechanisms (such as compositing and clustering techniques) have been developed (sections 2b and 2d). These make the comparison of model simulations with observations more stringent and more relevant for the evaluation of model cloud feedbacks.
- These new analyses give guidance on which dynamical regimes or cloud types are primarily responsible for the diversity of cloud feedbacks among models (section 2c). The responses of convective and boundary layer clouds both contribute to the spread of global cloud feedbacks in GCMs, with a dominant role of intermodel differences in the response of low-level clouds. The application to GCMs of observational tests focused on the response of boundary layer clouds to changes in large-scale environmental conditions (using observed climate variations not as an analog of long-term climate changes but as an example of changing environmental conditions) may thus help to determine which of the model cloud feedbacks are the more reliable. Relative confidence in the different model formulations can also be assessed against CRMs, as in the Global Energy and Water Cycle Experiment (GEWEX) Cloud System Study (GCSS; Randall et al. 2003).
- So far, only a small number of observational datasets [essentially the Earth Radiation Budget Experiment (ERBE; Barkstrom 1984) and ISCCP datasets] have been used widely to evaluate the GCMs' cloud properties and cloud radiative feedbacks. Indeed, over the last 20 yr we have been relying on passive radiometer retrievals that did not resolve cloud vertical structure (this latter had to be derived from field program radar measurements or radiosonde-based retrievals), and that mainly provided column-integrated or cloud-top retrieval products. The new A-Train constellation of satellites, that will include CloudSat and Calipso in particular (Stephens et al. 2002), will be the first real observational advance in cloud property retrievals in a long time: new observations from active spaceborne radar and lidar, in synergy with other instruments, will provide vertical profiles of multilayer cloud amount, cloud condensate, cloud phase properties, and microphysical size distributions and precipitation (Stephens et al. 2002). The use of new and existing observations of clouds, used together with the methodologies of model–data comparison presented in this paper, provide a foundation for future progress in our ability to evaluate cloud feedbacks in GCMs.

b. Water vapor–lapse rate feedbacks

The overall picture of the water vapor–lapse rate feedback under climate change—considered as the most positive climate feedback affecting climate sensitivity and associated, to a first approximation, with a nearly unchanged relative humidity—has remained fairly stable over time. Recent studies make us more confident in the reliability of this picture.

- Our understanding of the physical processes that control the relative humidity distribution (section 3a), as well as recent analyses of interannual to decadal climate variations (section 3b) and of the water vapor response to the Pinatubo eruption (section 3d), suggest that the mean tropospheric relative humidity may not undergo substantial changes as long as the large-scale atmospheric circulation remains largely unchanged. However, some uncertainty remains as to the role of cloud microphysical processes in the response of the tropospheric relative humidity distribution to climate warming.
- Currently there is no substantive evidence to suggest that, as a first approximation, the weak relative humidity response simulated under climate change is an artifact of GCMs (section 3e).
- It seems unlikely that the water vapor feedback associated with CO_2 forcing is substantially affected by changes in the lower-stratospheric water vapor (section 3f). But lower-stratospheric water vapor changes are likely to play a more important role in the climate response to other types of forcings (e.g., ozone).
- However, recent comparisons of the observed and simulated variations of water vapor and relative humidity in the current climate reveal biases in GCMs (sections 3c, 3d, and 3e), and there is still a nonnegligible spread in the model estimates of the water vapor–lapse rate feedback under climate change (Fig. 1). This spread is likely to result from intermodel differences in the meridional patterns of surface warming and in the magnitude (albeit small) of relative humidity changes.
- More quantitative investigations are thus required to determine *how accurately* the lapse rate and relative humidity variations (as well as their variations with surface temperature or other factors) need to be reproduced in the current climate to more rigorously constrain the magnitude of the water vapor–lapse rate feedback estimates under climate change.

c. Cryosphere feedbacks

The cryosphere is an important contributor to climate sensitivity through various feedbacks, in particu-

lar the snow/ice albedo feedbacks. However, the magnitude of these and other cryosphere-related feedbacks remains uncertain (Fig. 1). The cryospheric feedbacks in high latitudes are strongly coupled to processes in the atmosphere and in the ocean, particularly to polar cloud processes and ocean heat and freshwater transport. While some advances have been demonstrated in developing sea ice components of the coupled GCMs during the last few years, further progress is hampered by the scarcity of observational data in the polar regions, sea ice and snow thickness being currently a particular problem. Detailed satellite and in situ datasets should help to improve parameterizations of sea ice and snow processes, as well as their interaction with other components of the climate system. For instance, diagnostic tests have been proposed recently to evaluate the climate change snow albedo feedback produced by GCMs by using the Northern Hemisphere springtime warming and simultaneous snow retreat in the current seasonal cycle as an analog for anthropogenic climate change (section 4a). Development of an appropriate set of metrics allowing the testing against observations of the sea ice and snow parameterizations and their effect on climate sensitivity is needed on the way toward reducing uncertainties associated with the cryosphere feedbacks.

d. Final remarks

Recent studies have thus led to improvements in the identification of the reasons for differing global climate feedbacks among GCMs, and have given us clues on how we may evaluate the GCMs' feedbacks using observations. Many of the model–data diagnostics of comparison that have been developed over the last few years could now be applied to the ensemble of global climate models used for climate change projections. This, together with the use of new observational datasets, would improve our understanding of the origin of intermodel differences, and our assessment of the reliability of the climate feedbacks produced by the different GCMs. This paper also identifies many issues requiring further investigation. We are confident that continuing development in climate feedback research will produce an improved suite of techniques and of diagnostics to better understand and evaluate the physical processes that govern climate feedbacks at work in GCMs under global warming. Hopefully, this will lead to progress in narrowing the range of climate sensitivity estimates in the future.

APPENDIX A

How Are Feedbacks Defined?

The concept of feedback, which has long been used in electronics to characterize the behavior of a perturbed system (Bode 1945), is also used in climatology to characterize the response of the climate system to an external radiative forcing (Hansen et al. 1984).

Let T_s and R be the global mean surface temperature and the earth's radiation budget at the TOA: $R = (S_o/4)(1 - \alpha) - \text{OLR}$, where S_o, α and OLR are the insolation, the planetary albedo, and the TOA OLR, respectively. At equilibrium, $R = 0$. Let us assume now that an external perturbation, such as a change in the atmospheric concentration of carbon dioxide or in the solar constant, is imposed to the climate system and disequilibrates the earth's radiation budget by ΔQ (ΔQ is called a radiative forcing). The climate system responds to this radiative imbalance by changing its global mean temperature. At any time, the change (from its unperturbed equilibrium value) in global mean surface temperature ΔT_s can be related to the imposed radiative forcing and to the radiative imbalance at the TOA through the equation:

$$\Delta R = \Delta Q + \lambda \Delta T_s, \qquad \text{(A1)}$$

where λ is called the *feedback parameter* (note that fluxes are assumed positive downward). The climate system reaches a new equilibrium when $\Delta R = 0$.

As T_s changes, many climate variables change in concert. If these variables affect the OLR or the planetary albedo, their change has the potential to affect ΔR and thus the relationship between the magnitude of the imposed radiative forcing ΔQ and the magnitude of the climate response ΔT_s. In other words, they affect the climate feedback parameter λ.

Let x be a vector representing an ensemble of climate variables affecting R. A feedback parameter λ can be formally defined as

$$\lambda = \frac{\partial R}{\partial T_s} = \sum_x \frac{\partial R}{\partial x} \frac{\partial x}{\partial T_s} + \sum_x \sum_y \frac{\partial^2 R}{\partial x \partial y} \frac{\partial x \partial y}{\partial T_s^2} + \cdots$$

$$\text{(A2)}$$

The most fundamental feedback in the climate system is the temperature dependence of LW emission through

the Stefan–Boltzmann law of blackbody emission (Planck response). For this reason, the surface temperature response of the climate system is often compared to the response that would be obtained ($\Delta T_{s,P}$) if the temperature was the only variable to respond to the radiative forcing, and if the temperature change was horizontally and vertically uniform: $\Delta T_{s,P} = (\Delta R - \Delta Q)\lambda_P$. The global mean surface temperature change occurring when all the climate variables x respond to the change in T_s can then be expressed as $\Delta T_s = (\lambda_P/\lambda)\Delta T_{s,P}$. Since the feedback parameter is the sum of the Planck response (or Planck feedback parameter) and of all other feedbacks, one may write to first order (i.e., by neglecting the interaction between feedbacks): $\lambda = \lambda_P + \Sigma_{x \neq P}\lambda_x$, where $\lambda_x = (\partial R/\partial x)(\partial x/\partial T_s)$. Then the global surface temperature change can be expressed as

$$\Delta T_s = \frac{1}{1 - \sum_{x \neq P} g_x} \Delta T_{s,P}, \qquad (A3)$$

where $g_x = -(\lambda_x/\lambda_P)$ is called the *feedback gain* for the variable x, the feedback gain for all the variables $x \neq P$ being $g = \Sigma_{x \neq P} g_x$. The quantity $f = 1/(1 - g)$ is called the *feedback factor*. If g is positive (negative), $\Delta T_s \geq \Delta T_{s,P}$ ($\Delta T_s \leq \Delta T_{s,P}$, respectively). The Planck feedback parameter λ_P is negative (an increase in temperature enhances the LW emission to space and thus reduces R) and its typical value for the earth's atmosphere, estimated from GCM calculations[A1] (Colman 2003; Soden and Held 2006), is about -3.2 W m^{-2} K^{-1} (a value of -3.8 W m^{-2} K^{-1} is obtained by defining λ_P simply as $-4\sigma T^3$, by equating the global mean OLR to σT^4 and by assuming an emission temperature of 255 K). Therefore, for any variable $x \neq P$, the sign of the feedback gain g_x is the sign of the feedback parameter λ_x. On this convention, a positive (negative) feedback parameter thus amplifies (dampens) the temperature response of the climate system to a prescribed radiative forcing and enhances (reduces) the climate sensitivity.

APPENDIX B

How Are Global Radiative Feedbacks Diagnosed in GCMs?

Several approaches have been proposed to diagnose radiative feedbacks in GCMs. As reviewed by Soden et

---

[A1] Note that in GCM calculations, the Planck feedback parameter is usually estimated by perturbing in each grid box the tropospheric temperature at each level by the surface temperature change predicted under climate warming. Therefore this estimate does not correspond exactly to a vertically and horizontally uniform temperature change.

al. (2004) and Stephens (2005), each of these has its own strengths and weaknesses. Three main approaches are presented below.

a. The PRP approach

The partial radiative perturbation (PRP) method (Wetherald and Manabe 1988) evaluates partial derivatives of model TOA radiation with respect to changes in model parameters (such as water vapor, lapse rate, and clouds) by diagnostic rerunning of the model radiation code. It computes the feedback parameter of a variable x as $\lambda_x = (\partial R/\partial x)(dx/dT_s)$, and computes dx/dT_s by differencing the climate simulated at two different time periods. The feedback parameter computed through this method is close to its formal definition [(A2)], except that dx/dT_s is used instead of $\partial x/\partial T_s$, and that second-order terms (which represent interacting feedbacks) are often (but not always) neglected.

The advantage of this method is that it permits separate explicit evaluation of the radiative impact of the different feedbacks, and allows in particular the evaluation of the radiative impact of changes in clouds alone (Colman 2001; Soden et al. 2004). However, there are assumptions of linearity, and separability of the different feedbacks, meaning that the applicability of the method has been the subject of debate (Aires and Rossow 2003) and that caution must be applied in its interpretation. Furthermore, the radiative partial derivatives themselves cannot be validated against observations.

b. The CRF approach

A second approach, commonly called the "cloud forcing" analysis approach (e.g., Cess et al. 1990, 1996), diagnoses climate feedback parameters from changes in TOA clear-sky radiation (R_{clear}), along with changes in CRF (CRF = $R - R_{\text{clear}}$). If ΔQ is an external radiative forcing applied to the climate system, the climate feedback parameter is computed as

$$\lambda = \frac{\Delta R_{\text{clear}} - \Delta Q}{\Delta T_s} + \frac{\Delta \text{CRF}}{\Delta T_s}. \qquad (B1)$$

It is thus decomposed into clear-sky and cloudy components, the clear-sky component arising from combined temperature, water vapor, and surface albedo changes and the cloudy component from the change in the radiative impact of clouds. As discussed by Zhang et al. (1996), Colman (2003), and Soden et al. (2004), the magnitude (and sometimes the sign) of the cloud feedback parameter diagnosed by this method differs from that diagnosed by the PRP approach. This is because by definition the CRF characterizes the *contrast*

between clear-sky and cloudy radiation, and thus the so-called cloud feedback parameter $\Delta CRF/\Delta T_S$ depends on changes in both cloud and clear-sky (water vapor, temperature, surface albedo) properties, while the PRP method diagnoses cloud feedbacks from changes in cloud properties *only*.[B1] While the cloud feedback parameter computed through the CRF approach may thus be more difficult to interpret than that derived from PRP, its calculation is straightforward and therefore commonly performed from GCM simulations. Moreover, the CRF is directly observable and hence it may be validated in models' control climates.

c. The online feedback suppression approach

A third approach is to suppress one particular physical process (e.g., the radiative impact of water vapor changes) in a model, and then compare the model response with a standard model version (Hall and Manabe 1999; Schneider et al. 1999; Soden et al. 2002). Potential problems with this approach include the difficulty in separating processes within the model (Aires and Rossow 2003), the loss of short-scale and short-term correlations (e.g., between humidity and cloud cover), as well as problems with fixing highly nonlinear processes, such as clouds (Taylor and Ghan 1992; Schneider et al. 1999). However, it has the advantage of permitting an evaluation of the impact of feedbacks on variability over a broad range of time scales, in addition to climate change (Hall and Manabe 1999; Hall 2004), which permits direct comparison with observations (e.g., Soden et al. 2002).

d. Limits of these methods

A particular difficulty in the interpretation of feedback processes arises from the time scales of the different responses. Some processes participating in the feedback mechanisms may be very fast, some very slow. While the nonlinear equations fundamental to atmospheric GCMs cause a sensitivity to initial conditions that leads to chaotic behavior and a lack of predictability for weather events, there is little evidence for an equivalent degree of sensitivity to initial conditions and lack of predictability in predictions of temporally averaged climate variables from coupled GCMs. For this reason, climate feedbacks have traditionally been analyzed in terms of the new equilibria reached by the

system after a perturbation has been applied. This practice might however neglect important dynamical components of the response (Hallegatte et al. 2006). More recently, the time dependence of radiative feedbacks in coupled models has been investigated (Senior and Mitchell 2000; Boer and Yu 2003a), and some dynamical aspects of climate sensitivity have been examined by Boer and Yu (2003b).

Methods for separating the contributions from different radiative feedback processes do, by their nature, neglect nonradiative interactions between feedback processes. The PRP and CRF radiative feedback decomposition methods do not give any insight into, for example, the extent to which clouds may change in response to water vapor and evaporation increases as sea ice recedes in a warmer climate. There is no reason why such nonradiative interactions should necessarily scale with the global mean temperature change, and the appropriateness of using this as a control variable in feedback analysis has been challenged (Aires and Rossow 2003; Stephens 2005). However, the feedback suppression approach does allow nonradiative feedback interactions to be investigated, as has been shown in the analysis of vegetation feedbacks in palaeoclimate experiments (e.g., Braconnot et al. 1999).

The concept of feedback synergy, which can give a measure of the nonlinear interaction of different feedback processes, has been developed from the work of Stein and Alpert (1993), and has, for example, been applied with the feedback suppression method in a GCM by Braconnot et al. (1999). In the PRP context, nonlinearities in diagnosed global-scale radiative feedbacks have also been noted, for example in clouds and lapse rate feedbacks (Colman et al. 1997) and surface albedo feedback under increasingly large climate changes. For modest climate changes, however, a number of studies have noted that residuals obtained by PRP analysis suggest relatively small nonlinearities at the *global* scale, and a high degree of separability between the different radiative feedbacks (e.g., Mitchell and Ingram 1992; Colman et al. 1997; Soden et al. 2004).

In spite of their limitations, the different techniques have been useful in helping to improve our understanding of the role of different processes in determining overall model sensitivity, in structuring the discussion on climate sensitivity, and in permitting results to be shared and compared between models (e.g., Cess et al. 1990, 1996; Colman 2003a; Soden and Held 2006; WEBB; Winton 2006).

e. Decomposition of global radiative feedbacks

Some of these approaches have been applied to a wide range of GCMs (Colman 2003a; Soden and Held

---

[B1] A classic example is the following: a situation with a bright low cloud cover over equally bright sea ice might be associated with zero SW CRF. If the ice melting leads to a dark sea, the SW CRF becomes very large (giving a large SW cloud forcing anomaly) while the cloud has not changed.

2006; WEBB; Winton 2006). This makes it possible to compare the feedbacks produced by the different models and then to better interpret the spread of GCMs' estimates of climate sensitivity.

Neglecting nonlinearities and the interaction among feedbacks, the feedback parameter (A2) can be expressed as

$$\lambda = \lambda_P + \lambda_{LR} + \lambda_{WV} + \lambda_A + \lambda_C, \qquad (B2)$$

where λ_P, λ_{LR}, λ_{WV}, λ_A, and λ_C are the Planck feedback parameter (i.e., the feedback associated with changes in surface temperature, assuming that the tropospheric temperature change is vertically uniform and equal to the surface temperature change), and feedback parameters associated with changes in vertical temperature lapse rate, in water vapor, in surface albedo, and in clouds, respectively. Global estimates (derived from GCMs) of these different feedback parameters are shown in Fig. 1.

REFERENCES

Aires, F., and W. B. Rossow, 2003: Inferring instantaneous, multivariate and nonlinear sensitivities for the analysis of feedback processes in a dynamical system: Lorentz model casestudy. *Quart. J. Roy. Meteor. Soc.,* **129,** 239–275.

Alexeev, V., 2003: Sensitivity to CO_2 doubling of an atmospheric GCM coupled to an oceanic mixed layer: A linear analysis. *Climate Dyn.,* **20,** 775–787.

——, P. Langen, and J. Bates, 2005: Polar amplification of surface warming on an aquaplanet in "ghost forcing" experiments without sea ice feedbacks. *Climate Dyn.,* **24,** 655–666.

Allan, R. P., and A. Slingo, 2002: Can current climate forcings explain the spatial and temporal signatures of decadal OLR variations? *Geophys. Res. Lett.,* **29,** 1141, doi:10.1029/2001GL014620.

——, K. P. Shine, A. Slingo, and J. A. Pamment, 1999: The dependence of clear-sky outgoing longwave radiation on surface temperature and relative humidity. *Quart. J. Roy. Meteor. Soc.,* **125,** 2103–2126.

——, V. Ramaswamy, and A. Slingo, 2002: A diagnostic analysis of atmospheric moisture and clear-sky radiative feedback in the Hadley Centre and Geophysical Fluid Dynamics Laboratory (GFDL) climate models. *J. Geophys. Res.,* **107,** 4329, doi:10.1029/2001JD001131.

——, M. A. Ringer, and A. Slingo, 2003: Evaluation of moisture in the Hadley Centre climate model using simulations of HIRS water vapour channel radiances. *Quart. J. Roy. Meteor. Soc.,* **129,** 3371–3389.

Allen, M. R., and W. J. Ingram, 2002: Constraints on future changes in climate and the hydrologic cycle. *Nature,* **419,** 224–231.

Barkstrom, B. R., 1984: The Earth Radiation Budget Experiment (ERBE). *Bull. Amer. Meteor. Soc.,* **65,** 1170–1185.

Bates, J. J., and D. L. Jackson, 2001: Trends in upper-tropospheric humidity. *Geophys. Res. Lett.,* **28,** 1695–1698.

——, ——, F.-M. Breon, and Z. D. Bergen, 2001: Variability of tropical upper tropospheric humidity 1979–1998. *J. Geophys. Res.,* **106,** 32 271–32 281.

Bauer, M., A. D. Del Genio, and J. R. Lanzante, 2002: Observed and simulated temperature humidity relationships: Sensitivity to sampling and analysis. *J. Climate,* **15,** 203–215.

Betts, A. K., and Harshvardhan, 1987: Thermodynamic constraint on the cloud liquid water feedback in climate models. *J. Geophys. Res.,* **92,** 8483–8485.

Bitz, C. M., and G. H. Roe, 2004: A mechanism for the high rate of sea-ice thinning in the Arctic ocean. *J. Climate,* **17,** 3622–3631.

——, M. M. Holland, A. J. Weaver, and M. Eby, 2001: Simulating the ice-thickness distribution in a coupled climate model. *J. Geophys. Res.,* **106,** 2441–2463.

Blankenship, C., and T. T. Wilheit, 2001: SSM/T-2 measurements of regional changes in three-dimensional water vapour fields during ENSO events. *J. Geophys. Res.,* **106,** 5239–5254.

Bode, H., 1945: *Network Analysis and Feedback Amplifier Design.* Van Nostrand, 551 pp.

Boer, G. J., and B. Yu, 2003a: Climate sensitivity and climate state. *Climate Dyn.,* **21,** 167–176.

——, and ——, 2003b: Dynamical aspects of climate sensitivity. *Geophys. Res. Lett.,* **30,** 1135, doi:10.1029/2002GL016549.

Bony, S., and J.-L. Dufresne, 2005: Marine boundary layer clouds at the heart of tropical cloud feedback uncertainties in climate models. *Geophys. Res. Lett.,* **32,** L20806, doi:10.1029/2005GL023851.

——, J.-P. Duvel, and H. L. Treut, 1995: Observed dependence of the water vapor and clear-sky greenhouse effect on sea surface temperature; comparison with climate warming experiments. *Climate Dyn.,* **11,** 307–320.

——, K.-M. Lau, and Y. C. Sud, 1997: Sea surface temperature and large-scale circulation influences on tropical greenhouse effect and cloud radiative forcing. *J. Climate,* **10,** 2055–2077.

——, J.-L. Dufresne, H. LeTreut, J.-J. Morcrette, and C. Senior, 2004: On dynamic and thermodynamic components of cloud changes. *Climate Dyn.,* **22,** 71–86.

Braconnot, P., S. Joussaume, O. Marti, and N. de Noblet, 1999: Synergistic feedbacks from ocean and vegetation on the African monsoon response to mid-holocene insolation. *Geophys. Res. Lett.,* **26,** 2481–2484.

Bretherton, C., R. Ferrari, and S. Legg, 2004: Climate Process Teams: A new approach to improving climate models. *U.S. CLIVAR Var.,* **2,** 1–6.

——, P. N. Blossey, and M. E. Peters, 2006: Comparison of simple and cloud-resolving models of moist convection-radiation interaction with a mock-Walker circulation. *Theor. Comput. Fluid Dyn.,* in press.

Brogniez, H., R. Roca, and L. Picon, 2005: Evaluation of the distribution of subtropical free tropospheric humidity in AMIP-2 simulations using METEOSAT water vapor channel data. *Geophys. Res. Lett.,* **32,** L19708, doi:10.1029/2005GL024341.

Caldeira, K., A. K. Jain, and M. I. Hoffert, 2003: Climate sensitivity uncertainty and the need for energy without CO_2 emission. *Science,* **299,** 2052–2054.

Carnell, R., and C. Senior, 1998: Changes in mid-latitude variability due to increasing greenhouse gases and sulphate aerosols. *Climate Dyn.,* **14,** 369–383.

Cess, R. D., 1975: Global climate change: An investigation of atmospheric feedback mechanisms. *Tellus,* **27,** 193–198.

——, and Coauthors, 1990: Intercomparison and interpretation of cloud-climate feedback processes in nineteen atmospheric general circulation models. *J. Geophys. Res.,* **95,** 16 601–16 615.

——, and Coauthors, 1991: Interpretation of snow-climate feedback as produced by 17 general circulation models. *Science,* **253,** 888–892.

——, and Coauthors, 1996: Cloud feedback in atmospheric general circulation models: An update. *J. Geophys. Res.,* **101,** 12 791–12 794.

Chambers, L. H., B. Lin, and D. F. Young, 2002: Examination of new CERES data for evidence of tropical iris feedback. *J. Climate,* **15,** 3719–3726.

Chen, J., B. E. Carlson, and A. D. Del Genio, 2002: Evidence for strengthening of the tropical general circulation in the 1990s. *Science,* **295,** 838–841.

Clement, A. C., and R. Seager, 1999: Climate and the tropical oceans. *J. Climate,* **12,** 3383–3401.

——, and B. Soden, 2005: The sensitivity of the tropical-mean radiation budget. *J. Climate,* **18,** 3189–3203.

Colman, R., 2001: On the vertical extent of atmospheric feedbacks. *Climate Dyn.,* **17,** 391–405.

——, 2003: A comparison of climate feedbacks in general circulation models. *Climate Dyn.,* **20,** 865–873.

——, 2004: On the structure of water vapour feedbacks in climate models. *Geophys. Res. Lett.,* **31,** L21109, doi:10.1029/2004GL020708.

——, S. Power, and B. McAvaney, 1997: Non-linear climate feedback analysis in an atmospheric GCM. *Climate Dyn.,* **13,** 717–731.

Cotton, W. R., 1990: *Storms.* Geophysical Science Series, Vol. 1, *ASTeR Press, 158 pp.

Curry, J. A., W. B. Rossow, D. Randall, and J. L. Schramm, 1996: Overview of arctic cloud and radiation characteristics. *J. Climate,* **9,** 1731–1764.

——, J. L. Schramm, D. Perovich, and J. O. Pinto, 2001: Applications of SHEBA/FIRE data to evaluation of snow/ice albedo parameterizations. *J. Geophys. Res.,* **106** (D14), 15 345–15 355.

Dai, A., and K. E. Trenberth, 2004: The diurnal cycle and its depiction in the Community Climate System Model. *J. Climate,* **17,** 930–951.

Del Genio, A. D., and A. B. Wolf, 2000: The temperature dependence of the liquid water path of low clouds in the southern great plains. *J. Climate,* **13,** 3465–3486.

——, and W. Kovari, 2002: Climatic properties of tropical precipitating convection under varying environmnetal conditions. *J. Climate,* **15,** 2597–2615.

Dessler, A. E., and S. C. Sherwood, 2000: Simulations of tropical upper tropospheric humidity. *J. Geophys. Res.,* **105** (D15), 20 155–20 163.

Dickinson, R. E., G. A. Meehl, and W. M. Washington, 1987: Ice-albedo feedback in a CO_2-doubling simulation. *Climate Change,* **10,** 241–248.

Emanuel, K. A., 1994: *Atmospheric Convection.* Oxford University Press, 580 pp.

——, and R. T. Pierrehumbert, 1996: *Microphysical and Dynamical Control of Tropospheric Water Vapour.* Vol. 35, *Clouds, Chemistry and Climate,* NATO ASI Series, Springer-Verlag, 17–28.

——, and M. Zivkovic-Rothman, 1999: Development and evaluation of a convection scheme for use in climate models. *J. Atmos. Sci.,* **56,** 1766–1782.

——, J. D. Neelin, and C. Bretherton, 1994: On large-scale circulations in convecting atmospheres. *Quart. J. Roy. Meteor. Soc.,* **120,** 1111–1143.

Flato, G., 2004: Sea-ice and its response to CO_2 forcing as simulated by global climate models. *Climate Dyn.,* **23,** 229–241.

Folkins, I., K. K. Kelly, and E. M. Weinstock, 2002: A simple explanation for the increase in relative humidity between 11 and 14 km in the tropics. *J. Geophys. Res.,* **107,** 4736, doi:10.1029/2002JD002185.

Forster, P. M. D. F., and K. P. Shine, 1999: Stratospheric water vapour changes as a possible contributor to observed stratospheric cooling. *Geophys. Res. Lett.,* **26,** 3309–3312.

——, and M. Collins, 2004: Quantifying the water vapour feedback associated with post-Pinatubo cooling. *Climate Dyn.,* **23,** 207–214.

Fu, Q., M. Baker, and D. L. Hartmann, 2002: Tropical cirrus and water vapour: An effective Earth infrared iris? *Atmos. Chem. Phys.,* **2,** 31–37.

Fyfe, J. C., 2003: Extratropical Southern Hemisphere cyclones: Harbingers of climate change? *J. Climate,* **16,** 2802–2805.

Geng, Q., and M. Sugi, 2003: Possible change of extratropical cyclone activity due to enhanced greenhouse gases and sulfate aerosols—Study with a high-resolution AGCM. *J. Climate,* **16,** 2802–2805.

Gray, D. M., and P. G. Landine, 1987: Albedo model for shallow prairie snow covers. *Can. J. Earth Sci.,* **24,** 1760–1768.

Greenwald, T. J., G. L. Stephens, S. A. Christopher, and T. H. Vonder Haar, 1995: Observations of the global characteristics and regional radiative effects of marine cloud liquid water. *J. Climate,* **8,** 2928–2946.

Groisman, P., T. Karl, and R. Knight, 1994: Observed impact of snow cover on the heat balance and rise of continental spring temperatures. *Science,* **263,** 198–200.

Hall, A., 2004: The role of surface albedo feedback in climate. *J. Climate,* **17,** 1550–1568.

——, and S. Manabe, 1999: The role of water vapour feedback in unperturbed climate variability and global warming. *J. Climate,* **12,** 2327–2346.

——, and ——, 2000: Suppression of ENSO in a coupled model without water vapor feedback. *Climate Dyn.,* **16,** 393–403.

——, and X. Qu, 2006: Using the current seasonal cycle to constrain snow albedo feedback in future climate change. *Geophys. Res. Lett.,* **33,** L03502, doi:10.1029/2005GL025127.

Hall, N. M. J., B. J. Hoskins, P. J. Valdes, and C. A. Senior, 1994: Storm tracks in a high resolution GCM with doubled carbon dioxide. *Quart. J. Roy. Meteor. Soc.,* **120,** 1209–1230.

Hallegatte, S., A. Lahellec, and J.-Y. Grandpeix, 2006: An elicitation of the dynamic nature of water vapor feedback in climate change using a 1D model. *J. Atmos. Sci.,* **63,** 1878–1894.

Hansen, J., and L. Nazarenko, 2004: Soot climate forcing via snow and ice albedos. *Proc. Natl. Acad. Sci. USA,* **101,** 423–428.

——, A. Lacis, D. Rind, G. Russell, P. Stone, I. Fung, R. Ruedy, and J. Lerner, 1984: Climate sensitivity: Analysis of feedback mechanisms. *Climate Processes and Climate Sensitivity, Geophys. Monogr.,* Vol. 29, Amer. Geophys. Union, 130–163.

——, M. Sato, and R. Ruedy, 1997: Radiative forcing and climate response. *J. Geophys. Res.,* **102,** 6831–6864.

Harrison, E. F., P. Minnis, B. R. Barkstrom, V. Ramanathan, R. D. Cess, and G. G. Gibson, 1990: Seasonal variation of cloud radiative forcing derived from the Earth Radiation Budget Experiment. *J. Geophys. Res.,* **95,** 18 687–18 703.

Hartmann, D. L., and M. L. Michelsen, 1993: Large-scale effects on the regulation of tropical sea surface temperature. *J. Climate,* **6,** 2049–2062.

——, and K. Larson, 2002: An important constraint on tropical cloud-climate feedback. *Geophys. Res. Lett.,* **29,** 1951–1954.

——, and M. L. Michelsen, 2002: No evidence for Iris. *Bull. Amer. Meteor. Soc.,* **83,** 249–254.

——, M. Ockert-Bell, and M. Michelsen, 1992: The effect of cloud type on Earth's energy balance: Global analysis. *J. Climate,* **5,** 1281–1304.

——, L. A. Moy, and Q. Fu, 2001: Tropical convection and the energy balance at the top of the atmosphere. *J. Climate,* **14,** 4495–4511.

Held, I. M., 1993: Large-scale dynamics and global warming. *Bull. Amer. Meteor. Soc.,* **74,** 228–241.

——, and B. J. Soden, 2000: Water vapour feedback and global warming. *Annu. Rev. Energy Environ.,* **25,** 441–475.

Holland, M. M., and C. M. Bitz, 2003: Polar amplification of climate change in coupled models. *Climate Dyn.,* **21,** 221–232.

——, ——, and A. J. Weaver, 2001: The influence of sea ice physics on simulations of climate change. *J. Geophys. Res.,* **106,** 19 639–19 655.

——, ——, E. C. Hunke, W. H. Lipscomb, and J. L. Schramm, 2006: Influence of the sea ice thickness distribution on polar climate in CCSM3. *J. Climate,* **19,** 2398–2414.

Houghton, J. T., Y. Ding, D. J. Griggs, M. Noguer, P. J. van der Linden, X. Dai, K. Maskell, and C. A. Johnson, Eds., 2001: *Climate Change 2001: The Scientific Basis.* Cambridge University Press, 944 pp.

Houze, R. A. J., and P. V. Hobbs, 1982: Organization and structure of precipitating cloud systems. *Advances in Geophysics,* Vol. 24, Academic Press, 225–315.

Hu, H., R. J. Oglesby, and B. Saltzman, 2000: The relationship between atmospheric water vapor and temperature in simulations of climate change. *Geophys. Res. Lett.,* **27,** 3513–3516.

Iacono, M. J., J. S. Delamere, E. J. Mlawer, and S. A. Clough, 2003: Evaluation of upper tropospheric water vapor in the NCAR Community Climate Model, CCM3, using modeled and observed HIRS radiances. *J. Geophys. Res.,* **108,** 4037, doi:10.1029/2002JD002539.

Inamdar, A. K., V. Ramanathan, and N. G. Loeb, 2004: Satellite observations of the water vapor greenhouse effect and column longwave cooling rates: Relative roles of the continuum and vibration-rotation to pure rotation bands. *J. Geophys. Res.,* **109,** D06104, doi:10.1029/2003JD003980.

Ingram, W. J., 2002: On the robustness of the water vapor feedback: GCM vertical resolution and formulation. *J. Climate,* **15,** 917–921.

——, C. A. Wilson, and J. F. B. Mitchell, 1989: Modeling climate change: An assessment of sea ice and surface albedo feedbacks. *J. Geophys. Res.,* **94** (D6), 8609–8622.

Iwasa, Y., Y. Abe, and H. Tanaka, 2004: Global warming of the atmosphere in radiative-convective equilibrium. *J. Atmos. Sci.,* **61,** 1894–1910.

Jakob, C., and G. Tselioudis, 2003: Objective identification of cloud regimes in the tropical western Pacific. *Geophys. Res. Lett.,* **30,** 2082, doi:10.1029/2003GL018367.

Joshi, M. M., and K. P. Shine, 2003: A GCM study of volcanic eruptions as a cause of increased stratospheric water vapor. *J. Climate,* **16,** 3525–3534.

——, K. Shine, M. Ponater, N. Stuber, R. Sausen, and L. Li, 2003: A comparison of climate response to different radiative forcings in three general circulation models: Towards an improved metric of climate change. *Climate Dyn.,* **20,** 843–854.

Katzfey, J. J., and K. L. Mcinnes, 1996: GCM simulations of eastern Australian cutoff lows. *J. Climate,* **9,** 2337–2355.

Keith, D. W., 2000: Stratosphere-troposphere exchange: Infer-

ences from the isotopic composition of water vapor. *J. Geophys. Res.,* **105** (D12), 15 167–15 174.

Kelly, M. A., and D. A. Randall, 2001: A two-box model of a zonal atmospheric circulation in the Tropics. *J. Climate,* **14,** 3944–3964.

——, ——, and G. L. Stephens, 1999: A simple radiative-convective model with a hydrological cycle and interactive clouds. *Quart. J. Roy. Meteor. Soc.,* **125A,** 837–869.

Kiehl, J. T., 1994: On the observed near cancellation between longwave and shortwave cloud forcing in tropical regions. *J. Climate,* **7,** 559–565.

——, and P. R. Gent, 2004: The Community Climate System Model, Version 2. *J. Climate,* **17,** 3666–3682.

Klein, S. A., 1997: Synoptic variability of low-cloud properties and meteorological parameters in the subtropical trade wind boundary layer. *J. Climate,* **10,** 2018–2039.

——, and D. L. Hartmann, 1993: The seasonal cycle of low stratiform clouds. *J. Climate,* **6,** 1587–1606.

——, and C. Jakob, 1999: Validation and sensitivities of frontal clouds simulated by the ECMWF model. *Mon. Wea. Rev.,* **127,** 2514–2531.

Lambert, S. J., 1995: The effect of enhanced greenhouse gas warming on winter cyclone frequencies and strengths. *J. Climate,* **8,** 1447–1452.

Lapeyre, G., and I. M. Held, 2004: The role of moisture in the dynamics and energetics of turbulent baroclinic eddies. *J. Atmos. Sci.,* **61,** 1693–1710.

Larson, K., and D. L. Hartmann, 2003: Interactions among cloud, water vapor, radiation, and large-scale circulation in the tropical climate. Part I: Sensitivity to uniform sea surface temperature changes. *J. Climate,* **16,** 1425–1440.

——, ——, and S. A. Klein, 1999: The role of clouds, water vapor, circulation, and boundary layer structure in the sensitivity of the tropical climate. *J. Climate,* **12,** 2359–2374.

Lau, K.-M., C.-H. Ho, and M.-D. Chou, 1996: Water vapor and cloud feedback over tropical oceans: Can we use ENSO as a surrogate for climate change? *Geophys. Res. Lett.,* **23,** 2971–2974.

Lau, N.-C., and M. W. Crane, 1995: A satellite view of the synoptic-scale organization of cloud properties in midlatitude and tropical circulation systems. *Mon. Wea. Rev.,* **123,** 1984–2006.

——, and ——, 1997: Comparing satellite and surface observations of cloud patterns in synoptic-scale circulation systems. *Mon. Wea. Rev.,* **125,** 3172–3189.

L'Heveder, B., and M.-N. Houssais, 2001: Investigating the variability of the arctic sea ice thickness in response to a stochastic thermodynamic atmospheric forcing. *Climate Dyn.,* **17,** 107–125.

Lin, B., B. A. Wielicki, L. H. Chambers, Y. Hu, and K.-M. Xu, 2002: The Iris hypothesis: A negative or positive cloud feedback? *J. Climate,* **15,** 3–7.

——, T. Wong, B. A. Wielicki, and Y. Hu, 2004: Examination of the decadal tropical mean ERBS nonscanner radiation data for the Iris hypothesis. *J. Climate,* **17,** 1239–1246.

Lin, W. Y., and M. H. Zhang, 2004: Evaluation of clouds and their radiative effects simulated by the NCAR community atmospheric model against satellite observations. *J. Climate,* **17,** 3302–3318.

Lindzen, R. S., 1990: Some coolness concerning global warming. *Bull. Amer. Meteor. Soc.,* **71,** 288–299.

——, M. D. Chou, and A. Y. Hou, 2001: Does the Earth have an

adaptative infrared Iris? *Bull. Amer. Meteor. Soc.,* **82,** 417–432.

——, ——, and ——, 2002: Comments on "no evidence for Iris." *Bull. Amer. Meteor. Soc.,* **83,** 1345–1349.

Lohmann, U., and J. Feichter, 2005: Global indirect aerosol effects: A review. *Atmos. Chem. Phys.,* **5,** 715–737.

Luo, Z., and W. B. Rossow, 2004: Characterizing tropical cirrus life cycle, evolution, and interaction with upper-tropospheric water vapor using Lagrangian trajectory analysis of satellite observations. *J. Climate,* **17,** 4541–4563.

Manabe, S., and R. T. Wetherald, 1967: Thermal equilibrium of the atmosphere with a given distribution of relative humidity. *J. Atmos. Sci.,* **24,** 241–259.

——, and R. J. Stouffer, 1980: Sensitivity of a global climate model to an increase of CO_2 concentration in the atmosphere. *J. Geophys. Res.,* **85,** 5529–5554.

Marsden, D., and F. P. J. Valero, 2004: Observations of water vapor greenhouse absorption over the Gulf of Mexico using aircraft and satellite data. *J. Atmos. Sci.,* **61,** 745–753.

Maykut, G., 1982: Large-scale heat exchange and ice production in the central arctic. *J. Geophys. Res.,* **87,** 7971–7984.

McAvaney, B. J., and H. Le Treut, 2003: The cloud feedback model intercomparison project: CFMIP. *CLIVAR Exchanges*, No. 26 (Suppl.), International CLIVAR Project Office, Southampton, United Kingdom, 1–4.

McCabe, G. J., M. P. Clark, and M. C. Serreze, 2001: Trends in Northern Hemisphere surface cyclone frequency and intensity. *J. Climate,* **14,** 2763–2768.

McCarthy, M., and R. Toumi, 2004: Observed interannual variability of tropical troposphere relative humidity. *J. Climate,* **17,** 3181–3191.

Meehl, G. A., G. Boer, C. Covey, M. Latif, and R. Stouffer, 2000: The Coupled Model Intercomparison Project (CMIP). *Bull. Amer. Meteor. Soc.,* **81,** 313–318.

Miller, R. L., 1997: Tropical thermostats and low cloud cover. *J. Climate,* **10,** 409–440.

Minschwaner, K., and A. E. Dessler, 2004: Water vapor feedback in the tropical upper troposphere: Model results and observations. *J. Climate,* **17,** 1272–1282.

——, ——, and P. Sawaengphokhai, 2006: Multimodel analysis of the water vapor feedback in the tropical upper troposphere. *J. Climate,* in press.

Mitas, C. M., and A. Clement, 2005: Has the Hadley cell been strengthening in recent decades? *Geophys. Res. Lett.,* **32,** L03809, doi:10.1029/2004GL021765.

Mitchell, J. F. B., and W. J. Ingram, 1992: Carbon dioxide and climate: Mechanisms of changes in cloud. *J. Climate,* **5,** 5–21.

Moyer, E. J., F. W. Irion, Y. L. Yung, and M. Gunson, 1996: ATMOS stratospheric deuterated water and implications for troposphere-stratosphere transport. *Geophys. Res. Lett.,* **23,** 2385–2388.

Murphy, J., D. Sexton, D. Barnett, G. Jones, M. Webb, M. Collins, and D. Stainforth, 2004: Quantification of modelling uncertainties in a large ensemble of climate change simulations. *Nature,* **429,** 768–772.

Nolin, A. W., and J. Stroeve, 1997: The changing albedo of the Greenland ice sheet: Implications for climate modeling. *Ann. Glaciol.,* **25,** 51–57.

Norris, J. R., 1998a: Low cloud type over the ocean from surface observations. Part I: Relationship to surface meteorology and the vertical distribution of temperature and moisture. *J. Climate,* **11,** 369–382.

——, 1998b: Low cloud type over the ocean from surface observations. Part II: Geographical and seasonal variations. *J. Climate,* **11,** 383–403.

——, and S. A. Klein, 2000: Low cloud type over the ocean from surface observations. Part III: Relationship to vertical motion and the regional surface synoptic environment. *J. Climate,* **13,** 245–256.

——, and C. P. Weaver, 2001: Improved techniques for evaluating GCM cloudiness applied to the NCAR CCM3. *J. Climate,* **14,** 2540–2550.

——, and S. F. Iacobellis, 2005: North Pacific cloud feedbacks inferred from synoptic-scale dynamic and thermodynamic relationships. *J. Climate,* **18,** 4862–4878.

NRC, 2003: *Understanding Climate Change Feedbacks.* National Academies Press, 152 pp.

Paciorek, C. J., J. S. Risbey, V. Ventura, and R. D. Rosen, 2002: Multiple indices of Northern Hemisphere cyclone activity, winters 1949–99. *J. Climate,* **15,** 1573–1590.

Perovich, D. K., and Coauthors, 1999: *SHEBA: Snow and Ice Studies.* Cold Regions Research and Engineering Laboratory Tech. Rep., CD-ROM.

——, ——, ——, and P. V. Hobbs, 2002: Seasonal evolution of the albedo of multiyear Arctic sea ice. *J. Geophys. Res.,* **107,** 8044, doi:10.1029/2000JC000438.

Peters, M. E., and C. Bretherton, 2005: A simplified model of the Walker circulation with an interactive ocean mixed layer and cloud–radiative feedbacks. *J. Climate,* **18,** 4216–4234.

Pierrehumbert, R. T., 1995: Thermostats, radiator fins, and the local runaway greenhouse. *J. Atmos. Sci.,* **52,** 1784–1806.

——, and R. Roca, 1998: Evidence for control of Atlantic subtropical humidity by large scale advection. *Geophys. Res. Lett.,* **25,** 4537–4540.

Potter, G. L., and R. D. Cess, 2004: Testing the impact of clouds on the radiation budgets of 19 atmospheric general circulation models. *J. Geophys. Res.,* **109,** D02106, doi:10.1029/2003JD004018.

Qu, X., and A. Hall, 2005: Surface contribution to planetary albedo variability in cryosphere regions. *J. Climate,* **18,** 5239–5252.

——, and ——, 2006: Assessing snow albedo feedback in simulated climate change. *J. Climate,* **19,** 2617–2630.

Ramanathan, V., R. D. Cess, E. F. Harrison, P. Minnis, B. R. Barkstrom, and D. L. Hartmann, 1989: Cloud-radiative forcing and climate: Results from the Earth Radiation Budget Experiment. *Science,* **243,** 57–63.

Randall, D., and Coauthors, 1994: Analysis of snow feedbacks in 14 general circulation models. *J. Geophys. Res.,* **99,** 20 757–20 771.

——, and Coauthors, 2003: Confronting models with data: The GEWEX Cloud Systems Study. *Bull. Amer. Meteor. Soc.,* **84,** 455–469.

Rennó, N., K. A. Emanuel, and P. Stone, 1994: Radiative-convective model with an explicit hydrological cycle. Part I: Formulation and sensitivity to model parameters. *J. Geophys. Res.,* **99,** 14 429–14 441.

Rind, D., and P. Lonergan, 1995: Modelled impacts of stratospheric ozone and water vapour perturbations with implications for high-speed civil transport aircraft. *J. Geophys. Res.,* **100,** 7381–7396.

——, R. Healy, C. Parkinson, and D. Martinson, 1995: The role of sea ice in $2 \times CO_2$ climate model sensitivity. Part I: The total influence of sea ice thickness and extent. *J. Climate,* **8,** 449–463.

Ringer, M. A., and R. P. Allan, 2004: Evaluating climate model simulations of tropical clouds. *Tellus,* **56A,** 308–327.

Robock, A., 1983: Ice and snow feedbacks and the latitudinal and seasonal distribution of climate sensitivity. *J. Atmos. Sci.,* **40,** 986–997.

Rosenlof, K. H., 2003: How water enters the stratosphere. *Science,* **302,** 1691–1692.

——, A. F. Tuck, K. K. Kelly, J. M. Russell, and M. P. McCormick, 1997: Hemispheric asymmetries in water vapour and inferences about transport in the lower stratosphere. *J. Geophys. Res.,* **102,** 13 213–13 234.

Ross, R. J., W. P. Elliott, and D. J. Seidel, 2002: Lower-tropospheric humidity–temperature relationships in radiosonde observations and atmospheric general circulation models. *J. Hydrometeor.,* **3,** 26–38.

Rossow, W. B., and R. A. Schiffer, 1999: Advances in understanding clouds from ISCCP. *Bull. Amer. Meteor. Soc.,* **80,** 2261–2287.

Santer, B. D., and Coauthors, 2005: Amplification of surface temperature trends and variability in the tropical atmosphere. *Science,* **309,** 1551–1556.

Schneider, E. K., B. P. Kirtman, and R. S. Lindzen, 1999: Tropospheric water vapor and climate sensitivity. *J. Atmos. Sci.,* **56,** 1649–1658.

Senior, C. A., and J. F. B. Mitchell, 2000: The time dependence of climate sensitivity. *Geophys. Res. Lett.,* **27,** 2685–2688.

Sherwood, S. C., 1996: Maintenance of the free-tropospheric tropical water vapor distribution. Part II: Simulation by large-scale advection. *J. Climate,* **9,** 2919–2934.

——, and A. E. Dessler, 2000: On the control of stratospheric humidity. *Geophys. Res. Lett.,* **27,** 2513–2516.

Shine, K. P., and A. Sinha, 1991: Sensitivity of the earth's climate to height dependent changes in the water vapor mixing ratio. *Nature,* **354,** 382–384.

Sinclair, M., and I. Watterson, 1999: Objective assessment of extratropical weather systems in simulated climates. *J. Climate,* **12,** 3467–3485.

Slingo, A., K. I. Hodges, and G. J. Robinson, 2004: Simulation of the diurnal cycle in a climate model and its evaluation using data from Meteosat 7. *Quart. J. Roy. Meteor. Soc.,* **130,** 1449–1467.

Sobel, A. H., I. M. Held, and C. S. Bretherton, 2002: The ENSO signal in tropical tropospheric temperature. *J. Climate,* **15,** 2702–2706.

Soden, B. J., 2000: The sensitivity of the tropical hydrological cycle to ENSO. *J. Climate,* **13,** 538–549.

——, 2004: The impact of tropical convection and cirrus on upper tropospheric humidity: A Lagrangian analysis of satellite measurements. *Geophys. Res. Lett.,* **31,** L20104, doi:10.1029/2004GL020980.

——, and S. R. Schroeder, 2000: Decadal variations in tropical water vapor. *J. Climate,* **13,** 3337–3341.

——, and I. M. Held, 2006: An assessment of climate feedbacks in coupled ocean–atmosphere models. *J. Climate,* **19,** 3354–3360.

——, R. Wetherald, G. Stenchikov, and A. Robock, 2002: Global cooling after the eruption of Mount Pinatubo: A test of climate feedback by water vapor. *Science,* **296,** 727–730.

——, A. J. Broccoli, and R. S. Hemler, 2004: On the use of cloud forcing to estimate cloud feedback. *J. Climate,* **17,** 3661–3665.

Somerville, R. C. J., and L. A. Remer, 1984: Cloud optical thickness feedbacks in the CO_2 climate problem. *J. Geophys. Res.,* **89,** 9668–9672.

Spelman, M. J., and S. Manabe, 1984: Influence of oceanic heat transport upon the sensitivity of a model climate. *J. Geophys. Res.,* **89,** 571–586.

Spencer, R. W., and W. D. Braswell, 1997: How dry is the tropical free troposphere? Implications for global warming theory. *Bull. Amer. Meteor. Soc.,* **78,** 1097–1106.

Stainforth, D., and Coauthors, 2005: Uncertainty in predictions of the climate response to rising levels of greenhouse gases. *Nature,* **429,** 768–772.

Stein, U., and P. Alpert, 1993: Factor separation in numerical simulations. *J. Atmos. Sci.,* **50,** 2107–2115.

Stephens, G. L., 2005: Cloud feedbacks in the climate system: A critical review. *J. Climate,* **18,** 237–273.

——, and Coauthors, 2002: The CloudSat mission and the A-train: A new dimension of space-based observations of clouds and precipitation. *Bull. Amer. Meteor. Soc.,* **83,** 1771–1790.

Stocker, T., and Coauthors, 2001: Physical climate processes and feedbacks. *Climate Change 2001: The Scientific Basis,* J. T. Houghton et al., Eds., Cambridge University Press, 419–470.

Stone, P. H., and J. H. Carlson, 1979: Atmospheric lapse rate regimes and their parameterization. *J. Atmos. Sci.,* **36,** 415–423.

Stowasser, M., K. Hamilton, and G. J. Boer, 2006: Local and global climate feedbacks in models with differing climate sensitivities. *J. Climate,* **19,** 193–209.

Stuber, N., M. Ponater, and R. Sausen, 2001: Is the climate sensitivity to ozone perturbations enhanced by stratospheric water vapor feedback? *Geophys. Res. Lett.,* **28,** 2887–2890.

Sun, D.-Z., C. Covey, and R. S. Lindzen, 2001: Vertical correlations of water vapor in GCMs. *Geophys. Res. Lett.,* **28,** 259–262.

Taylor, K. E., and S. J. Ghan, 1992: An analysis of cloud liquid water feedback and global climate sensitivity in a general circulation model. *J. Climate,* **5,** 907–919.

Thorndike, A., D. S. Rothrock, G. Maykut, and R. Colony, 1975: The thickness distribution of sea ice. *J. Geophys. Res.,* **80,** 4501–4513.

Tian, B., B. J. Soden, and X. Wu, 2004: Diurnal cycle of convection, clouds and water vapor in the tropical upper troposphere: Satellites versus a general circulation model. *J. Geophys. Res.,* **109,** D10101, doi:10.1029/2003JD004117.

Tompkins, A. M., and G. C. Craig, 1999: Sensitivity of tropical convection to sea surface temperature in the absence of large-scale flow. *J. Climate,* **12,** 462–476.

——, and K. A. Emanuel, 2000: Simulated equilibrium tropical temperature and water vapor profiles and their sensitivity to vertical resolution. *Quart. J. Roy. Meteor. Soc.,* **126,** 1219–1238.

Trenberth, K. E., J. Fasullo, and L. Smith, 2005: Trends and variability in column-integrated atmospheric water vapour. *Climate Dyn.,* **24,** 741–758.

Tselioudis, G., and W. B. Rossow, 1994: Global, multiyear variations of optical thickness with temperature in low and cirrus clouds. *Geophys. Res. Lett.,* **21,** 2211–2214.

——, and C. Jakob, 2002: Evaluation of midlatitude cloud properties in a weather and a climate model: Dependence on dynamic regime and spatial resolution. *J. Geophys. Res.,* **107,** 4781, doi:10.1029/2002JD002259.

——, and W. B. Rossow, 2006: Climate feedback implied by observed radiation and precipitation changes with midlatitude storm strength and frequency. *Geophys. Res. Lett.,* **33,** L02704, doi:10.1029/2005GL024513.

——, A. Del Genio, W. Kovari Jr., and M.-S. Yao, 1998: Temperature dependence of low cloud optical thickness in the

GISS GCM: Contributing mechanisms and climate implications. *J. Climate,* **11,** 3268–3281.

——, Y.-C. Zhang, and W. R. Rossow, 2000: Cloud and radiation variations associated with northern midlatitude low and high sea level pressure regimes. *J. Climate,* **13,** 312–327.

Tsushima, Y., and S. Manabe, 2001: Influence of cloud feedback on annual variation of global mean surface temperature. *J. Geophys. Res.,* **106** (D19), 22 635–22 646.

——, A. Abe-Ouchi, and S. Manabe, 2005: Radiative damping of annual variation in global mean surface temperature: Comparison between observed and simulated feedback. *Climate Dyn.,* **24,** 591–597.

Vavrus, S., 2004: The impact of cloud feedbacks on Arctic climate under greenhouse forcing. *J. Climate,* **17,** 603–615.

Volodin, E. M., 2004: Relation between the global-warming parameter and the heat balance on the Earth's surface at increased contents of carbon dioxide. *Izv. Atmos. Oceanic Phys.,* **40,** 269–275.

Wallace, J. M., and R. V. Hobbs, 1977: *Atmospheric Science: An Introductory Survey.* Academic Press, 467 pp.

Washington, W. W., and G. A. Meehl, 1986: General circulation model CO_2 sensitivity experiments: Snow-sea ice albedo parameterizations and globally averaged surface air temperature. *Climate Change,* **8,** 231–241.

Weaver, C. P., 2003: Efficiency of storm tracks, an important climate parameter? The role of cloud radiative forcing in poleward heat transport. *J. Geophys. Res.,* **108,** 4018, doi:10.1029/2002JD002756.

——, and V. Ramanathan, 1996: The link between summertime cloud radiative forcing and extratropical cyclones in the North Pacific. *J. Climate,* **9,** 2093–2109.

Webb, M., C. Senior, S. Bony, and J.-J. Morcrette, 2001: Combining ERBE and ISCCP data to assess clouds in the Hadley Centre, ECMWF and LMD atmospheric climate models. *Climate Dyn.,* **17,** 905–922.

——, and Coauthors, 2006: On the contribution of local feedback mechanisms to the range of climate sensitivity in two GCM ensembles. *Climate Dyn.,* **27,** 17–38.

Webster, C. R., and A. J. Heymsfield, 2003: Water isotope ratios D/H, $^{18}O/^{16}O$, $^{17}O/^{16}O$ in and out of clouds map dehydration pathways. *Science,* **302,** 1742–1746.

Wentz, F. J., and M. Schabel, 2000: Precise climate monitoring using complementary satellite data sets. *Nature,* **403,** 414–416.

Wetherald, R., and S. Manabe, 1988: Cloud feedback processes in a general circulation model. *J. Atmos. Sci.,* **45,** 1397–1415.

Wielicki, B. A., and Coauthors, 2002: Evidence for large decadal variability in the tropical mean radiative energy budget. *Science,* **295,** 841–844.

Williams, K. D., M. A. Ringer, and C. A. Senior, 2003: Evaluating the cloud response to climate change and current climate variability. *Climate Dyn.,* **20,** 705–721.

——, and Coauthors, 2006: Evaluation of a component of the cloud response to climate change in an intercomparison of climate models. *Climate Dyn.,* **145,** 145–165.

Winton, M., 2006: Surface albedo feedback estimates for the AR4 climate models. *J. Climate,* **19,** 359–365.

Wood, R., and C. S. Bretherton, 2006: On the relationship between stratiform low cloud cover and lower tropospheric stability. *J. Climate,* in press.

Wu, X., W. D. Hall, W. W. Grabowski, M. W. Moncrieff, W. D. Collins, and J. T. Kiehl, 1999: Long-term behavior of cloud systems in TOGA COARE and their interactions with radiative and surface processes. Part II: Effects of ice microphysics on cloud–radiation interaction. *J. Atmos. Sci.,* **56,** 3177–3195.

Wyant, M. C., C. S. Bretherton, J. T. Bacmeister, J. T. Kiehl, I. M. Held, M. Z. Zhao, S. A. Klein, and B. J. Soden, 2006: A comparison of tropical cloud properties and responses in GCMs using mid-tropospheric vertical velocity. *Climate Dyn.,* in press.

Xu, K.-M., and K. A. Emanuel, 1989: Is the tropical atmosphere conditionally unstable? *Mon. Wea. Rev.,* **117,** 1471–1479.

Yang, F., A. Kumar, W. Wang, H. Juang, and M. Kanamitsu, 2001: Snow-albedo feedback and seasonal climate variability over North America. *J. Climate,* **14,** 4245–4248.

——, ——, M. E. Schlesinger, and W. Wang, 2003: Intensity of hydrological cycles in warmer climates. *J. Climate,* **16,** 2419–2423.

Yang, G.-Y., and J. Slingo, 2001: The diurnal cycle in the Tropics. *Mon. Wea. Rev.,* **129,** 784–801.

Yao, M.-S., and A. D. Del Genio, 2002: Effects of cloud parameterization on the simulation of climate changes in the GISS GCM. Part II: Sea surface temperature and cloud feedbacks. *J. Climate,* **15,** 2491–2503.

Yin, H., 2005: A consistent poleward shift of the storm tracks in simulations of 21st century climate. *Geophys. Res. Lett.,* **32,** L18701, doi:10.1029/2005GL023684.

Yu, W., M. Doutriaux, G. Sèze, H. L. Treut, and M. Desbois, 1996: A methodology study of the validation of clouds in GCMs using ISCCP satellite observations. *Climate Dyn.,* **12,** 389–401.

Yulaeva, E., and J. M. Wallace, 1994: The signature of ENSO in global temperature and precipitation fields derived from the microwave sounding unit. *J. Climate,* **7,** 1719–1736.

Zhang, M. H., J. J. Hack, J. T. Kiehland, and R. D. Cess, 1994: Diagnostic study of climate feedback processes in atmospheric general circulation models. *J. Geophys. Res.,* **99,** 5525–5537.

——, and Coauthors, 2005: Comparing clouds and their seasonal variations in 10 atmospheric general circulation models with satellite measurements. *J. Geophys. Res.,* **110,** D15S02, doi:10.1029/2004JD005021.

Zhang, Y.-C., and W. B. Rossow, 1997: Estimating meridional energy transports by the atmospheric and oceanic general circulations using boundary fluxes. *J. Climate,* **10,** 2358–2373.